doi:10.1093/brain/awr099 Brain 2011: 134; 3011–3029 | 3011

BRAIN
A JOURNAL OF NEUROLOGY

White matter damage in primary progressive aphasias: a diffusion tensor tractography study

Sebastiano Galantucci,[1,2] Maria Carmela Tartaglia,[1] Stephen M. Wilson,[1,3] Maya L. Henry,[1] Massimo Filippi,[2] Federica Agosta,[2] Nina F. Dronkers,[4,5] Roland G. Henry,[6] Jennifer M. Ogar,[1] Bruce L. Miller[1] and Maria Luisa Gorno-Tempini[1,7]

1 Memory and Ageing Centre, Department of Neurology, University of California San Francisco, San Francisco, CA 94143, USA
2 Neuroimaging Research Unit, Institute of Experimental Neurology, Division of Neuroscience, Scientific Institute and University Hospital San Raffaele, Milan, Italy
3 Department of Speech Language and Hearing Sciences, Department of Neurology, University of Arizona, Tucson, AZ 85721, USA
4 Center for Aphasia and Related Disorders, VA Northern California Health Care System, Martinez, CA 94553, USA
5 Department of Neurology, University of California, Davis, Davis, CA 95616, USA
6 Department of Radiology and Biomedical Imaging, University of California, San Francisco, San Francisco CA 94107, USA
7 Centre for Mind/Brain Sciences (CiMeC), University of Trento, Trento, Italy

Correspondence to: Maria Luisa Gorno-Tempini,
Memory and Ageing Centre,
Department of Neurology,
University of California,
San Francisco, 350 Parnassus Avenue,
Suite 905, San Francisco,
CA 94143-1207, USA
E-mail: marilu@memory.ucsf.edu

Primary progressive aphasia is a clinical syndrome that encompasses three major phenotypes: non-fluent/agrammatic, semantic and logopenic. These clinical entities have been associated with characteristic patterns of focal grey matter atrophy in left posterior frontoinsular, anterior temporal and left temporoparietal regions, respectively. Recently, network-level dysfunction has been hypothesized but research to date has focused largely on studying grey matter damage. The aim of this study was to assess the integrity of white matter tracts in the different primary progressive aphasia subtypes. We used diffusion tensor imaging in 48 individuals: nine non-fluent, nine semantic, nine logopenic and 21 age-matched controls. Probabilistic tractography was used to identify bilateral inferior longitudinal (anterior, middle, posterior) and uncinate fasciculi (referred to as the ventral pathway); and the superior longitudinal fasciculus segmented into its frontosupramarginal, frontoangular, frontotemporal and temporoparietal components, (referred to as the dorsal pathway). We compared the tracts' mean fractional anisotropy, axial, radial and mean diffusivities for each tract in the different diagnostic categories. The most prominent white matter changes were found in the dorsal pathways in non-fluent patients, in the two ventral pathways and the temporal components of the dorsal pathways in semantic variant, and in the temporoparietal component of the dorsal bundles in logopenic patients. Each of the primary progressive aphasia variants showed different patterns of diffusion tensor metrics alterations: non-fluent patients showed the greatest changes in fractional anisotropy and radial and mean diffusivities; semantic variant patients had severe changes in all metrics; and logopenic patients had the least white matter damage, mainly involving diffusivity, with fractional anisotropy altered only in the temporoparietal component of the dorsal pathway. This study demonstrates that both careful dissection of the main language tracts and consideration of all diffusion tensor metrics are necessary to characterize the white matter changes that occur in the variants of primary progressive aphasia. These results highlight the potential value of diffusion tensor imaging as a new tool in the multimodal diagnostic evaluation of primary progressive aphasia.

Received December 1, 2010. Revised March 17, 2011. Accepted March 28, 2011. Advance Access publication June 11, 2011

Keywords: primary progressive aphasia; progressive non-fluent aphasia; semantic dementia; logopenic progressive aphasia; diffusion tensor imaging

Abbreviations: DTI = diffusion tensor imaging; SLF = superior longitudinal fasciculus

Introduction

Primary progressive aphasia is a clinical syndrome characterized by progressive, isolated impairment of language functions (Mesulam, 1982, 2001). Aphasic symptoms are caused by gradual degeneration of different parts of the language network. Three main clinical variants of primary progressive aphasia have been described depending on which parts of this network have the greatest damage: (i) non-fluent/agrammatic primary progressive aphasia (previously called progressive non-fluent aphasia) is characterized by agrammatism, motor speech errors and left inferior frontal damage; (ii) semantic variant primary progressive aphasia (previously called semantic dementia) is characterized by single-word comprehension and retrieval deficits, loss of semantic knowledge, surface dyslexia and anterior temporal atrophy; and (iii) the logopenic variant primary progressive aphasia (previously called logopenic progressive aphasia) is characterized by word-finding deficits, phonological errors in spontaneous speech and naming, sentence repetition impairment and left posterior temporal and inferior parietal damage (Hodges and Patterson, 1996; Neary *et al*., 1998; Gorno-Tempini *et al*., 2004, 2008; Mesulam *et al*., 2009; Rabinovici and Miller, 2010; Henry and Gorno-Tempini, 2010). Primary progressive aphasia is considered one of the possible clinical manifestations of frontotemporal lobar degeneration-type pathologies, although Alzheimer's disease can also be found. There is no perfect phenotype–pathological relationship, but the most common distribution is a tauopathy or less frequently TDP-43 (type 3 Sampathu) in the non-fluent variant, TDP-43 (type 1 Sampathu) changes in the semantic variant, and Alzheimer's disease pathology in the logopenic variant (Davies *et al*., 2005; Josephs *et al*., 2006, 2008; Knibb *et al*., 2006; Mesulam *et al*., 2008).

Primary progressive aphasia neuroimaging research has focused primarily on grey matter damage and much less is known about white matter changes in primary progressive aphasia and frontotemporal dementia-related disorders. Diffusion tensor tractography is a novel technique that allows *in vivo* localization and reconstruction of white matter fibre tracts based on the diffusion properties of water in the white matter of the brain (Yamada *et al*., 2009). Due to the highly organized white matter structure, water cannot diffuse freely but has the tendency to diffuse preferentially in a direction parallel to the longitudinal axis of the axons. This phenomenon is called water-diffusion anisotropy (or directionality) and can be represented by the diffusion tensor model (Basser *et al*., 1994; Hagmann *et al*., 2006; Assaf and Pasternak, 2008; Yamada *et al*., 2009). The tensor has three eigenvalues; the largest, $\lambda 1$ is called axial diffusivity (or parallel, $\lambda //$) and is parallel to the axonal direction. The two smaller ones are called $\lambda 2$ and $\lambda 3$ and are averaged to provide a measure of radial diffusivity (or perpendicular) ($\lambda \perp$). These parameters can be averaged to provide a mean diffusivity and can be used to compute the fractional anisotropy, which is a scalar value that describes the shape of the diffusion tensor and ranges from 0 to 1 (Basser *et al*., 1994). Axial and radial diffusivities are considered to be influenced by specific pathological processes underlying neurological disease and can provide valuable information. Specifically, alterations of axial diffusivity suggest axonal damage and alterations of radial diffusivity suggest myelin damage (Beaulieu, 2002; Song *et al*., 2002), although this remains controversial (Wheeler-Kingshott and Cercignani, 2009).

To our knowledge, only a few studies have used diffusion tensor imaging (DTI) to analyse changes occurring in the white matter of the patients with primary progressive aphasia and frontotemporal dementia. One study investigated non-fluent and semantic variant using DTI with a region of interest-based approach (Whitwell *et al*., 2010). Other studies (Matsuo *et al*., 2008; Agosta *et al*., 2009; Zhang *et al*., 2009) showed that DTI is able to detect and quantify microstructural changes in the white matter of patients with semantic, non-fluent or behavioural variant frontotemporal dementia, and that these patients were different from normal controls or patients with Alzheimer's disease. There are no DTI studies comparing all three variants of primary progressive aphasias, a deficiency that this article addresses.

We employed probabilistic DTI tractography to reconstruct specific white matter tracts and compared measures of microstructural alterations in the tracts among the different disease groups and controls. We chose this approach instead of a whole-brain, voxel-wise techniques because of its ability to reconstruct specific white matter pathways allowing the measurement of DTI metrics in the tracts of interest. Our aim was to determine if different primary progressive aphasia variants are associated with specific patterns of white matter damage. We hypothesized that each variant would have a specific anatomical localization of damage, involving tracts that originate from or connect with the brain regions shown to be atrophic in previous volumetric studies investigating primary progressive aphasia variants (Gorno-Tempini *et al*., 2004). We also hypothesized that we would identify a specific pattern of DTI metrics change since different pathological and biological processes are associated with each clinical phenotype.

Materials and methods

Subjects

Patients with primary progressive aphasia and healthy age-matched control subjects were recruited through the Memory and Ageing Centre at University of California San Francisco (UCSF). All participants or their surrogates gave written informed consent, and the study was approved by the UCSF institutional review board. Patients and controls received a comprehensive evaluation including history and neurological examination, neuropsychological testing and neuroimaging. A diagnosis of primary progressive aphasia required progressive, isolated

deterioration of speech and/or language functions in the first stages of the disease. Patients were then diagnosed with a particular primary progressive aphasia variant based on diagnostic classification recently developed by an international group of primary progressive aphasia researchers (Gorno-Tempini *et al*., 2011). Patients with previous or current history of other neurological, psychiatric and major medical conditions or a history of substance abuse were excluded. The sample included 48 participants: non-fluent ($n = 9$); semantic ($n = 9$); logopenic ($n = 9$); and normal controls ($n = 21$).

To assess the consistency of the atrophy pattern of the three primary progressive aphasia variants in our sample compared with previous reports, a voxel-based morphometry analysis was performed using the SPM5 software package (http://www.fil.ion.ucl.ac.uk/spm) (Ashburner and Friston, 2005) and a diffeomorphic exponentiated lie algebra (DARTEL) registration method (Ashburner, 2007), as previously described by Wilson *et al*. (2009). The total intracranial volume was determined using SPM5. The three primary progressive aphasia variants each showed left-lateralized atrophy (Supplementary Fig. 1). The regional distribution of tissue loss was consistent with previous studies (Mummery *et al*., 2000; Gorno-Tempini *et al*., 2004; Wilson *et al*., 2009).

Fifteen of these patients (six non-fluents, one semantic, eight logopenics) also underwent PET scanning with administration of Pittsburgh compound B to assess the presence of cortical amyloid binding. PET images with ^{11}C-Pittsburgh compound B were acquired and analysed as previously described (Rabinovici *et al*., 2007). Among the patients who successfully underwent the procedure, 7/8 logopenic patients were Pittsburgh compound B-positive, while none of the non-fluent patients and none of the semantic variant patients were Pittsburgh compound B-positive. One non-fluent patient had an equivocal reading of the PET-Pittsburgh compound B results.

Magnetic resonance image acquisition

MRI scans were acquired on a 3 T Siemens TrioTim syngo with an eight-channel transmit and receive head coil. A high-resolution 3D T_1-weighted image was acquired with the following parameters: 160 contiguous sagittal slices with 1 mm thickness; repetition time/echo time = 2300/2.98 ms; inversion time = 900 ms; flip angle = 9; field of view = 256 mm^2; matrix = 256 × 240; voxel size 1.0 × 1.0 × 1.0 mm^3. A FLAIR sequence was acquired as well, to exclude the presence of significant vascular disease in the subjects. The parameters were the following: 160 contiguous sagittal slices with 1 mm thickness; repetition time/echo time = 6000/389 ms; inversion time = 2100 ms; flip angle = 120; field of view = 256 mm^2; matrix = 256 × 258; voxel size 1.0 × 1.0 × 1.0 mm^3.

DTI was based on single-shot spin-echo echo-planar images with axial slices covering the whole brain supplemented with an Array Spatial Sensitivity Encoding Technique (ASSET) with a parallel imaging factor of 2 and consisting of 55 interleaved slices with 2.2 mm thickness; repetition time/echo time = 8000 ms/109 ms; flip angle = 90; field of view = 220 mm^2; matrix = 220 × 220; voxel size = 2.2 × 2.2 × 2.2 mm^3; number of acquisitions = 1. Diffusion gradients were applied in 64 directions uniformly distributed on a sphere through electrostatic repulsion with $b_0 = 2000$ s/mm^2.

Diffusion tensor imaging analysis

DTI analysis was performed using the FMRIB software library tools (http://www.fmrib.ox.ac.uk/fsl/fdt/index.html).

Preprocessing

The T_1- and diffusion-weighted data were skull stripped using the Brain Extraction Tool, removing all the non-brain tissue and aligned to MNI space using linear and non-linear registration. All Brain Extraction Tool results were visually inspected and, when needed, manual adjustments were performed to correct skull stripping errors. The T_1-weighted scans were then segmented into grey matter, white matter and CSF using FMRIB's Automated Segmentation Tool tissue-type segmentation within the FMRIB software library and partial volume maps were obtained. The diffusion-weighted data were registered using an affine registration to the b_0 volume to correct for eddy currents and motion artefacts.

Region of interest definition

We defined seeds for tractography in the native diffusion space on the fractional anisotropy and colour-coded maps. These regions of interest were defined manually by S.G. on coronal or axial slices based on *a priori* knowledge of the anatomy of the tracts and were localized where these tracts are known to pass through a bottleneck so all or most of the fibres constituting the tract could be included in the starting seed for tractography. Tractography was then performed using a single-seed approach. In order to exclude fibres from neighbouring tracts, we used exclusion masks for some tracts in areas of the brain where the specific tracts are known not to project.

The regions of interest for the tracts of interest were drawn as follows (an example on a single subject is illustrated in Fig. 1A):

(i) Inferior longitudinal fasciculus: a single starting seed region of interest was drawn in the temporal white matter on a coronal slice, posterior to a plane that was tangent to the anterior surface of the cerebral peduncles. We outlined only the lateral inferior white matter with an anterior–posterior directionality (green on colour-coded maps).

(ii) Uncinate fasciculus: a single region of interest was drawn on an axial slice in the region of transition from the anterior temporal lobe to the frontal orbital cortex, inferior to the anterior part of the external capsule. The region of interest was outlined on the cranio-caudally oriented white matter that is known to constitute the uncinate fasciculus and that appears blue in the colour-coded maps. In this case, we used two exclusion masks. The first one was on the middle sagittal slice and was designed to exclude commissural fibres such as the anterior commissure that connects the two hemispheres and passes very close to the uncinate fasciculus. The second exclusion mask was drawn on the same plane as the inferior longitudinal fasciculus starting seed region of interest and was designed to exclude all the fibres projecting from the inferior longitudinal fasciculus that enter the anterior temporal lobe and could interfere with the tracking of the uncinate fasciculus.

(iii) Superior longitudinal fasciculus (SLF): a single seed consisting of one region of interest drawn on the coronal slice posterior to the postcentral gyrus. The region of interest included fibres oriented in an anterior–posterior direction that were lateral to the cranio-caudally oriented white matter of the corona radiata and medial to the cortex. This region is considered to be a bottleneck for the SLF where all its components have to pass in order to reach their destination (Makris *et al*., 2005; Catani and Thiebaut de Schotten, 2008; Glasser and Rilling, 2008). For this tract, we used an exclusion mask located on the internal and external capsule in order to avoid interference from the corona radiata.

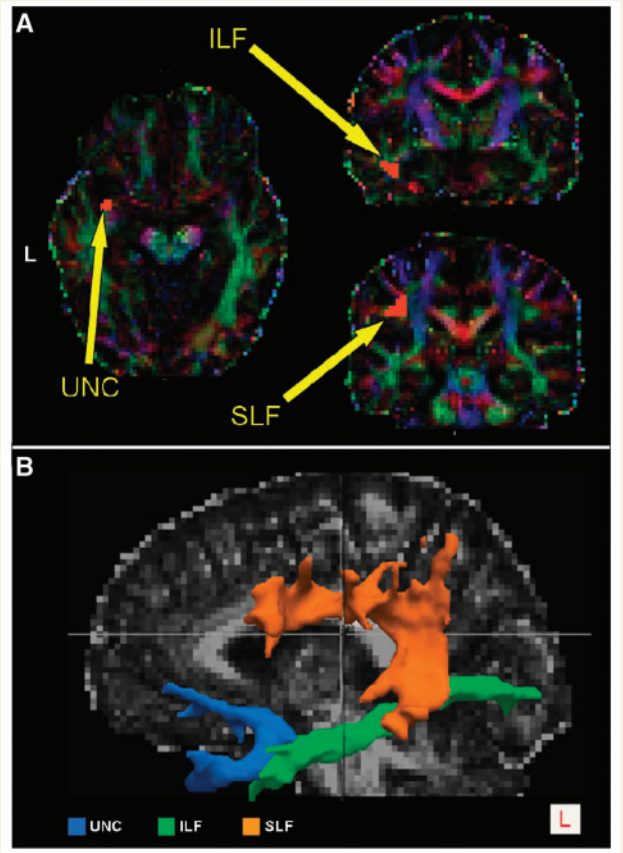

Figure 1 (**A**) Examples of the seeds defined for the left inferior longitudinal fasciculus, SLF and uncinate fasciculus, for a single subject. The regions of interest used as seeds are shown overlaid on the colour-coded maps in DTI native space, which show the principal direction of water diffusivity in white matter. Green was assigned to anterior–posterior, red to left–right and blue to craniocaudal white matter fibres. (**B**) 3D reconstructions of white matter tracts in a single healthy control. Left superior longitudinal fasciculus (SLF), inferior longitudinal fasciculus (ILF) and uncinate fasciculus (UNC) tracts are superimposed onto the subject's fractional anisotropy map. L = left.

Tract partitioning

Inferior longitudinal fasciculus partitioning

The inferior longitudinal fasciculus is a long ventral tract that connects the anterior temporal lobe with the ipsilateral occipital lobe. The relatively focal grey matter degeneration observed in prior studies (Gorno-Tempini *et al*., 2008; Brambati *et al*., 2009) in the anterior temporal lobe in the semantic variant and in the posterior temporal areas in the logopenic variant suggested that we partition the inferior longitudinal fasciculus along the anterior–posterior axis, in order to avoid diluting effects of averaging the DTI metrics over the whole tract. We divided the inferior longitudinal fasciculus into three parts (anterior, middle and posterior), and measured the DTI metrics separately for each inferior longitudinal fasciculus subdivision to investigate whether damage differed along the tract or was equally distributed. The partitioning was performed by dividing the tract, transformed to MNI space, on a coronal plane. We used the border between the splenium and the body of corpus callosum ($y = -25$) and the anterior commissure ($y = -8$) as the anatomical landmarks. We then transformed the partitioned tracts back into native space and recalculated DTI metrics for anterior, middle and posterior inferior longitudinal fasciculus and redid the statistical analysis.

The sub-components of the superior longitudinal fasciculus

The left SLF is a long, dorsal tract connecting fundamental regions within the language network (Makris *et al*., 1997; Catani *et al*., 2002). Five components have been described, which are likely to subserve different language functions, such as phonological, lexical retrieval and articulation of speech (Croxson *et al*., 2005; Makris *et al*., 2005; Friederici *et al*., 2006). Three superior components consisting of anterior–posterior fibres connect the superior parietal lobule (SLF-I), the angular gyrus (SLF-II) and the supramarginal gyrus (SLF-III) to ipsilateral frontal and opercular areas (Croxson *et al*., 2005; Makris *et al*., 2005; Rilling *et al*., 2008). An inferior component consists of fibres that connect the superior and middle temporal gyri to ipsilateral frontal areas and is commonly called the arcuate fasciculus or SLF-IV. Finally, a fifth temporoparietal component (SLF-tp), connects the inferior parietal lobe with the posterior temporal lobe, and has been described in several previous studies (Catani *et al*., 2005; Frey *et al*., 2008; Makris *et al*., 2009), although there remains some controversy about the nomenclature and the functional significance of this tract. Assuming that each component of the SLF connects different brain areas, we hypothesized that different primary progressive aphasia variants could be associated with damage to different components of the SLF and by assessing the SLF as a whole, focal injury might be overlooked because of averaging over the entire tract. Therefore, we tracked SLF-II, SLF-III, arcuate fasciculus and SLF-tp, which are the components associated with language function. The SLF-II, SLF-III and arcuate fasciculus components were reconstructed using a single seed with target approach. For SLF-tp, a double-seed approach was used.

The methodology for partitioning the SLF in its different components is less established than the tractography of the entire tracts (Catani *et al*., 2005; Makris *et al*., 2005). The whole-tract bundles are in fact easily identified in the fractional anisotropy and colour-coded maps (Fig. 1A). Instead, the division into specific branches relies more heavily on cortically dependent region of interest positioning. This is particularly true for the identification of the different SLF parietal components where there is a lack of objective anatomical boundaries between the posterior temporal, angular and supramarginal regions. For SLF partitioning, we therefore defined the seeds and the targets for the tractography in the MNI space according to the Harvard–Oxford probabilistic atlas (http://www.cma.mgh.harvard.edu/). This atlas provides probability maps of each cortical or subcortical structure in which each voxel has an absolute value that ranges from 0 to 100 representing the percentage of subjects who have that voxel in common for that region within the atlas. We then thresholded the obtained regions of interest at 30, so that each voxel included was represented in at least 30% of the subjects from which the atlas was obtained. This threshold was chosen based on the overlap of the regions of interest with the anatomical regions in the template, avoiding overlap with nearby areas that could bias the tractography results. Moreover, we restricted the seed regions of interest to the grey matter and one voxel of underlying white matter to avoid including unwanted tracts in the region of interest and to increase the specificity of the tractography results.

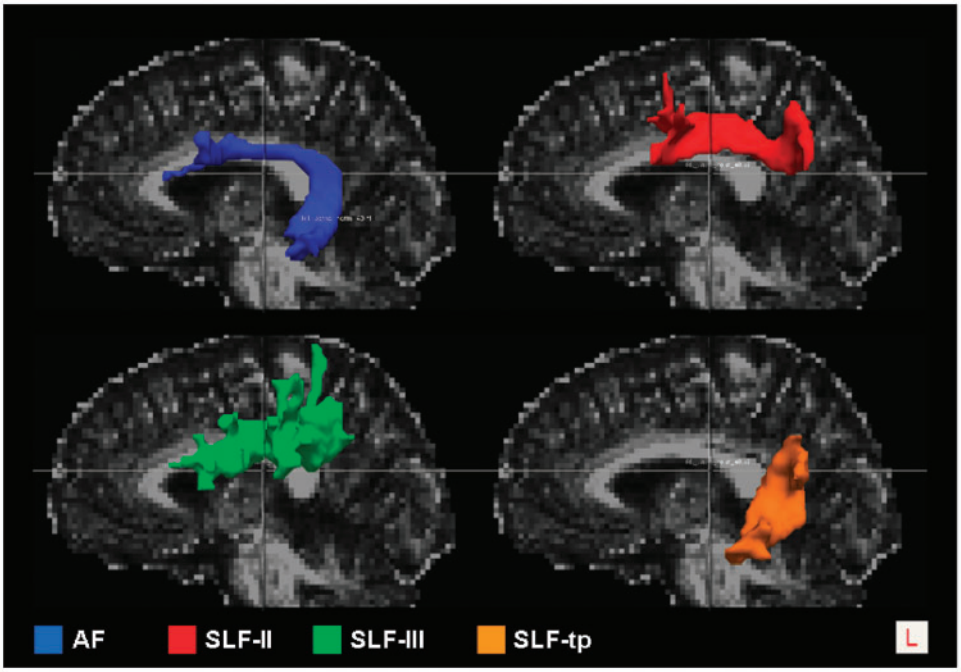

Figure 2 3D Reconstructions of left SLF components in a single healthy control. Left arcuate fasciculus (AF), frontoangular SLF (SLF-II), frontosupramarginal SLF (SLF-III), temporoparietal SLF (SLF-tp) tracts are overlaid onto the subject's fractional anisotropy map. L = left.

The seed regions of interest were established as follows: in the angular gyrus for SLF-II, in the supramarginal gyrus for SLF-III and in the posterior middle and superior temporal gyri for the arcuate fasciculus. For these components of the SLF, the target region of interest covered the whole ipsilateral frontal lobe. For the SLF-tp, the two seeds were placed in the angular gyrus and in the posterior middle and superior temporal gyri and were used alternatively as seed and target by the tractography algorithm. The seeds and targets were transformed to each subject's native diffusion space, by means of the inverse of the linear and non-linear transformations previously described and then binarized.

Regions of interest verification

A two-step procedure was adopted to check the correct positioning of all the regions of interest before running tractography. First, all seeds and targets that were drawn in native DTI space (entire tracts) or transformed from the standard to the diffusion space (SLF partitions) by a mean diffusivity with extensive neuroanatomical experience (S.G.), were also visually assessed and confirmed by two experienced neurologists (M.C.T. and M.L.G.-T.). A consensus was reached when there was not agreement on the anatomical location of the region of interests. This procedure was repeated on each patient's T_1-weighted scan transformed to the DTI space, in order to verify the cortical positioning of each region of interest on an image that allows better visualization of grey matter.

Fibre tracking

Fibre tracking was performed using a probabilistic tractography algorithm implemented in FSL (probtrackx) and based on Bayesian estimation of diffusion parameters (Bedpostx), following the method previously described by Behrens *et al*. (2003, 2007). Fibre tracking was initiated from all voxels within the seed masks in the diffusion space to generate 5000 streamline samples, with a step length of 0.5 mm and a curvature threshold of 0.2. Each tract was run separately for the right and left hemisphere. Fibre tracking resulted in a probabilistic map of the connections of the voxels included in the starting seed with the rest of the brain. Each voxel in the tract map had an intensity value that represented the number of tractography runs that were successfully able to pass in that voxel. The number of successful tractography runs was extremely high in the tract and extremely low outside the tract. The highest possible intensity value was represented by 5000, multiplied by the number of voxels in the starting seed, from which was subtracted the number of tracks that entered an exclusion mask and so excluded from the seeding set. The tract maps were normalized taking into consideration the number of voxels in the seed masks. To do so, the number of streamline samples present in the voxels in the tract maps was divided by the way-total, which corresponds to the total number of streamline samples that were not rejected due to exclusion masks. The obtained tract masks were thresholded to a value equal to 40% of the 95th percentile of the distribution of the intensity values in the voxels included in the tract. The normalization allowed us to correct for possible differences between tracts due to different dimensions of the starting seeds. In this way, it was also possible to exclude the background noise and avoid a too restrictive thresholding in case the maximum intensity value was an outlier of the distribution. An example of the tract reconstructions on a single subject is shown in Figs 1B and 2.

We generated probabilistic maps of the overlapping tracts and averaged the tract maps reconstructed from each single subject to investigate the consistency of distribution of the identified pathways across the subjects, and the anatomical accuracy of each tract (Figs 3 and 4). Group probability maps for each tract were also created to investigate the consistency of the tractography results among the different groups of subjects (Supplementary Figs 2 and 3).

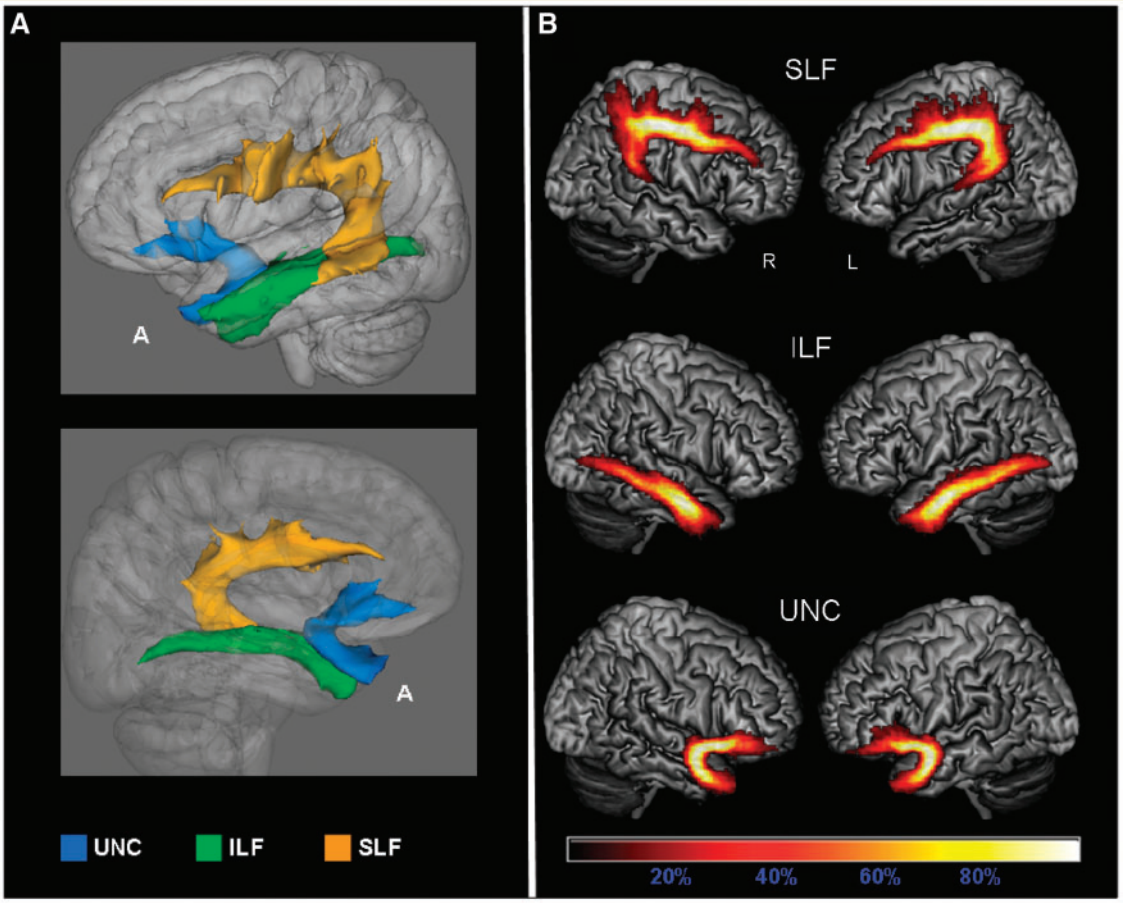

Figure 3 Probabilistic maps of the language-related tracts from all the subjects included in the study. The tracts are overlaid on a 3D rendering of the MNI standard brain. Only voxels present in at least 10% of the subjects are shown. (**A**) 3D reconstruction of all-subjects probability maps of left superior longitudinal fasciculus (SLF), inferior longitudinal fasciculus (ILF) and uncinate fasciculus (UNC) seen from left (*top*) and right (*bottom*). (**B**) All-subjects probability maps of bilateral SLF, inferior longitudinal fasciculus and uncinate fasciculus. The colour scale indicates the degree of overlap among subjects. A = anterior.

For each subject's tracts in native space, we calculated the axial diffusivity ($\lambda//$) defined as the largest eigenvalue, and the radial diffusivity ($\lambda\perp$), defined as the average of the minor eigenvalues. Axial and radial diffusivities were then averaged, obtaining mean diffusivity. Fractional anisotropy was calculated from the standard deviation of the three eigenvalues ranging from 0 to 1 (Basser *et al*., 1994). Group probability maps were then used to mask the fractional anisotropy and mean diffusivity maps, which were previously warped to a MNI template, and graphically display fractional anisotropy and mean diffusivity values in the voxels included in the probability maps (Figs 5–8).

Statistical analysis

The statistical analyses of demographic, cognitive data and DTI metric were performed using SPSS software (SPSS Inc). For demographic and cognitive data, Pearson χ^2-test or univariate ANOVAs were used to compare the different groups. Bonferroni corrections were performed for multiple comparisons.

For the statistical analysis of DTI metrics, average fractional anisotropy, mean diffusivity, $\lambda//$ and $\lambda\perp$ values were obtained from each subject's tracts, in native DTI space and entered in the statistical analysis. We compared fractional anisotropy, mean diffusivity, $\lambda//$ and $\lambda\perp$ values between the different groups, using a univariate ANCOVA model with Bonferroni correction for multiple comparisons. Age, gender and total intracranial volume were included in the model as covariates.

Since the clinical dementia rating box score was significantly higher in the semantic variant group, indicating increased severity, we repeated the statistical analysis, including the clinical dementia rating box score as a covariate. The general pattern of the results did not change indicating that dementia severity was not the primary determinant of the differences in DTI metrics.

In order to measure the influence of atrophy on DTI results, we repeated the statistical analysis adding the Jacobian coefficients along the tracts probability maps as covariates in our model. These coefficients are obtained during the non-linear registration on the MNI standard template and are a measure of how much the non-linear registration algorithm had to stretch or shrink the tracts from each patient to fit them to the template. We entered only the coefficients calculated from the non-linear part of the transformation in the model, in order to avoid head size bias. Jacobian coefficients were calculated voxel per voxel and the mean of the values obtained from the voxels included in the tracts probability maps was entered in the statistical

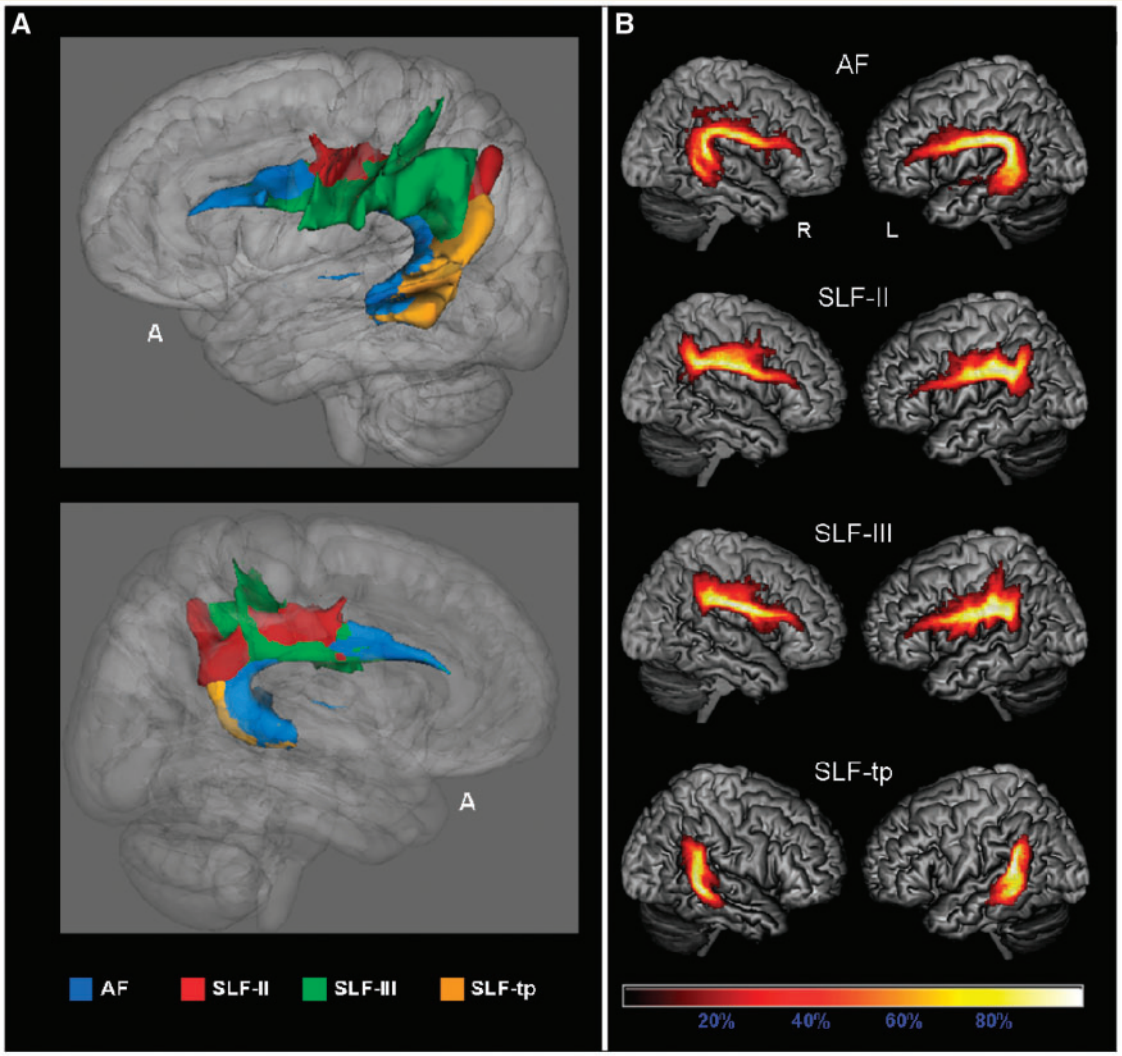

Figure 4 Subcomponents of the superior longitudinal fasciculus (SLF): all-subjects probability maps**.** The tracts are overlaid on a 3D rendering of the MNI standard brain. Only voxels present in at least 10% of the subjects are showed. (**A**) 3D reconstruction of left Arcuate fasciculus (AF), frontoangular SLF (SLF-II), frontosupramarginal SLF (SLF-III), temporoparietal SLF (SLF-tp) seen from left (*top*) and right (*bottom*). (**B**) All-subjects probability maps of bilateral arcuate fasciculus, SLF-II, SLF-III and SLF-tp. The colour scale indicates the degree of overlap among subjects.

model. After including the Jacobian determinants in the statistical model, the general pattern of DTI results was still conserved.

Results

Demographic and cognitive data

Demographic, clinical and language features of our sample are summarized in Table 1. There was no significant difference among the four groups for age, sex, education and handedness. The three primary progressive aphasia groups did not differ significantly from one another with respect to Mini-Mental State Examination score, or disease duration. Clinical dementia rating box score was significantly higher in the semantic variant group (Table 1).

Cognitive and language function results are shown in Tables 2 and 3, respectively. Every disease group showed the typical pattern of neuropsychological deficits that has been previously associated with each primary progressive aphasia variant (Gorno-Tempini *et al*., 2004; Wilson *et al*., 2009). The non-fluent variant showed greater deficits in motor speech and grammar; the semantic variant showed preserved fluency with severe naming, word comprehension and semantic processing; and the logopenic variant showed intermediate fluency, preserved word comprehension and semantics, and impaired repetition.

Diffusion tensor imaging: tract-specific metrics

Group differences in regional fractional anisotropy, mean diffusivity, $\lambda//$ and $\lambda\perp$ values, are summarized in Tables 4–7, respectively.

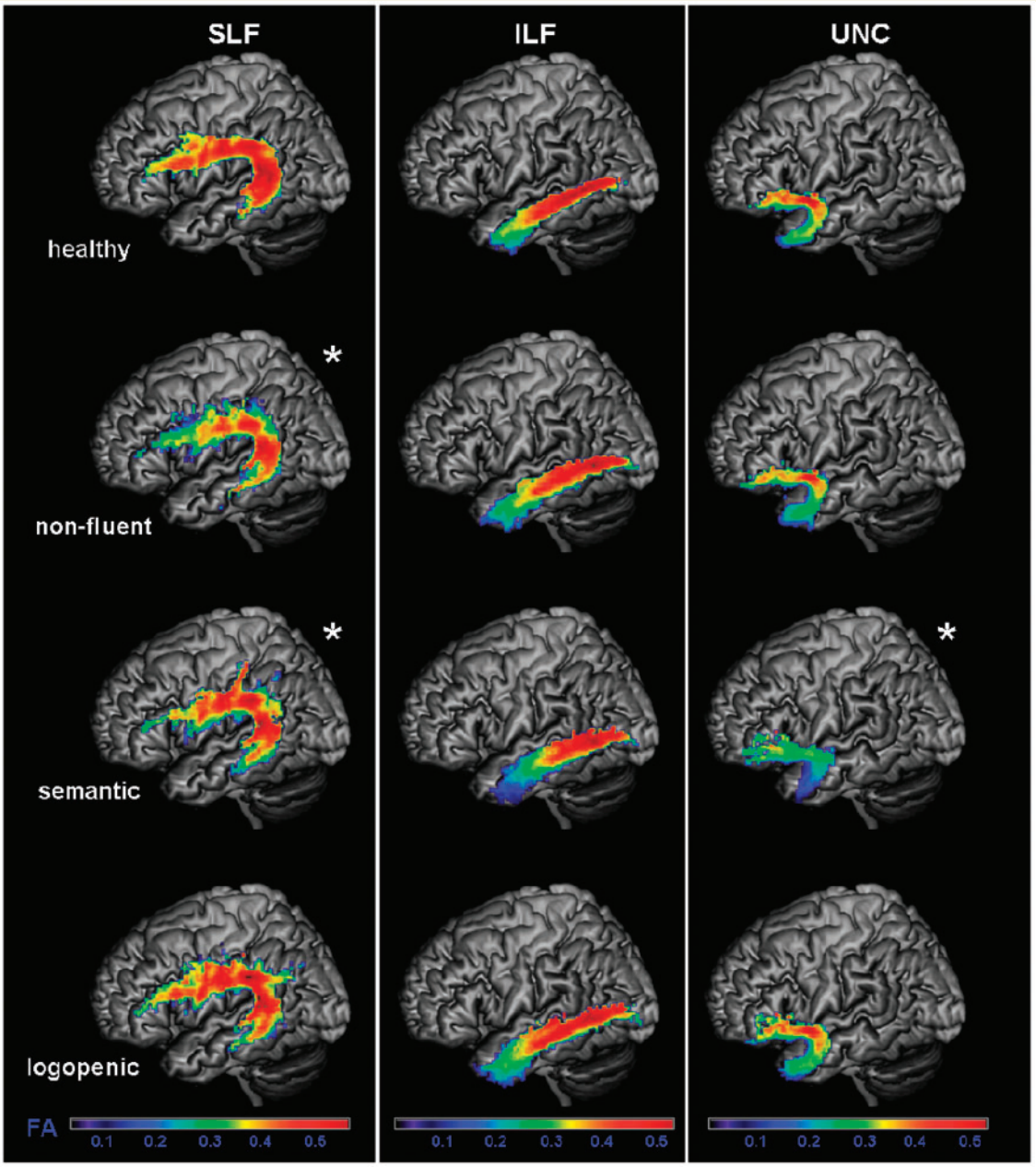

Figure 5 Fractional anisotropy (FA) values of each group in the probability maps for left superior longitudinal fasciculus (SLF), inferior longitudinal fasciculus (ILF), uncinate fasciculus (UNC), overlaid on a standard MNI brain. Only voxels that are in common in at least 20% of the subjects in each group were included in the probability maps. Asterisk denotes significantly different relative to normal controls at $P < 0.05$. The chromatic scale represents average fractional anisotropy values ranging from lower (violet–blue) to higher values (yellow–red).

Non-fluent variant

Patients with the non-fluent variant, when compared with healthy controls, showed significantly lower fractional anisotropy in the entire left SLF (Fig. 5), and in all the left-sided SLF components (Fig. 7). Mean diffusivity was significantly increased in all the left-sided SLF components except SLF-tp, while the $\lambda\perp$ was increased in all the left-sided SLF components (Figs 6 and 8). $\lambda//$ was not significantly different from controls. In contrast to these dorsal tracts, the ventral tracts connecting the temporal lobe to the occipital lobe or to the orbitofrontal cortex were spared (i.e. inferior longitudinal fasciculus and uncinate fasciculus).

In summary, non-fluent patients showed changes in DTI metrics (with the exception of $\lambda//$) in the left dorsal language pathways connecting frontoparietal or frontotemporal regions, but not in ventral tracts connecting the temporal lobe to the occipital lobe or to the orbitofrontal cortex. In some components of these dorsal tracts, non-fluent patients showed greater fractional anisotropy changes than logopenics and patients with the semantic variant.

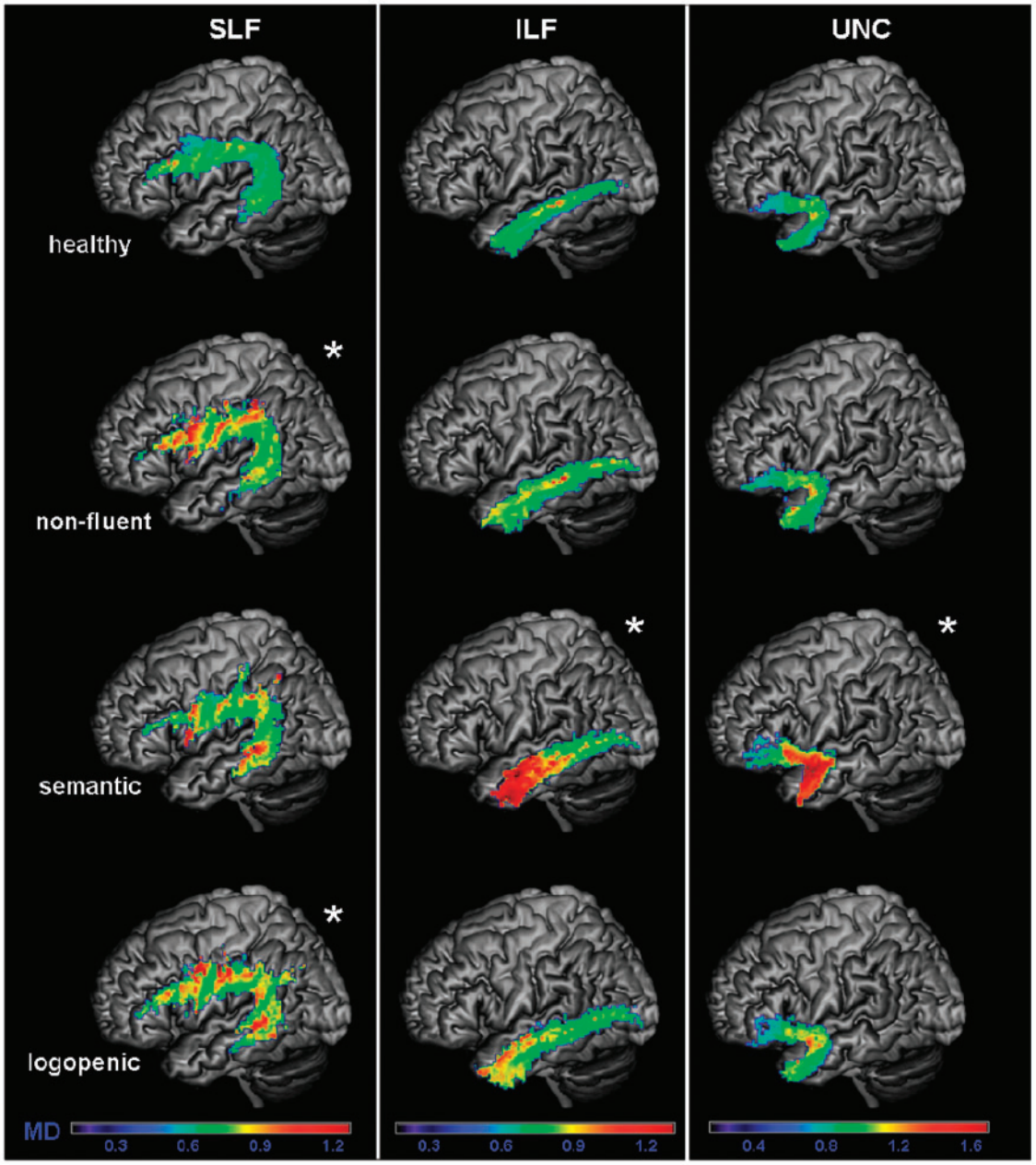

Figure 6 Mean diffusivity (MD) values of each group in the probability maps for left superior longitudinal fasciculus (SLF), inferior longitudinal fasciculus (ILF), uncinate fasciculus (UNC), overlaid on a standard MNI brain. Only voxels that are in common in at least 20% of the subjects in each group were included in the probability maps. Asterisk denotes significantly different relative to normal controls at $P < 0.05$. The chromatic scale represents average mean diffusivity values ranging from lower (violet–blue) to higher values (yellow–red). MD is measured in $mm^2/s \times 10^{-3}$.

Semantic variant

When entire tracts were considered, patients with the semantic variant showed altered DTI metrics in the uncinate fasciculus and in the inferior longitudinal fasciculus bilaterally, with an increase of diffusivities and a reduction of fractional anisotropy in the uncinate fasciculus and an increase of diffusivities without reduction of fractional anisotropy in the inferior longitudinal fasciculus (Figs 5 and 6). Within the inferior longitudinal fasciculus, the anterior portion showed lower fractional anisotropy bilaterally, while the middle portion was altered only on the left. Mean diffusivity, $\lambda//$ and $\lambda\perp$ were increased in the same regions in which fractional anisotropy was decreased.

Within the SLF, altered DTI metrics, in terms of reduced fractional anisotropy and increased diffusivities were noted only when considering the tracts' different components. In particular, the left arcuate fasciculus and the left SLF-tp were significantly different from controls (Figs 7 and 8).

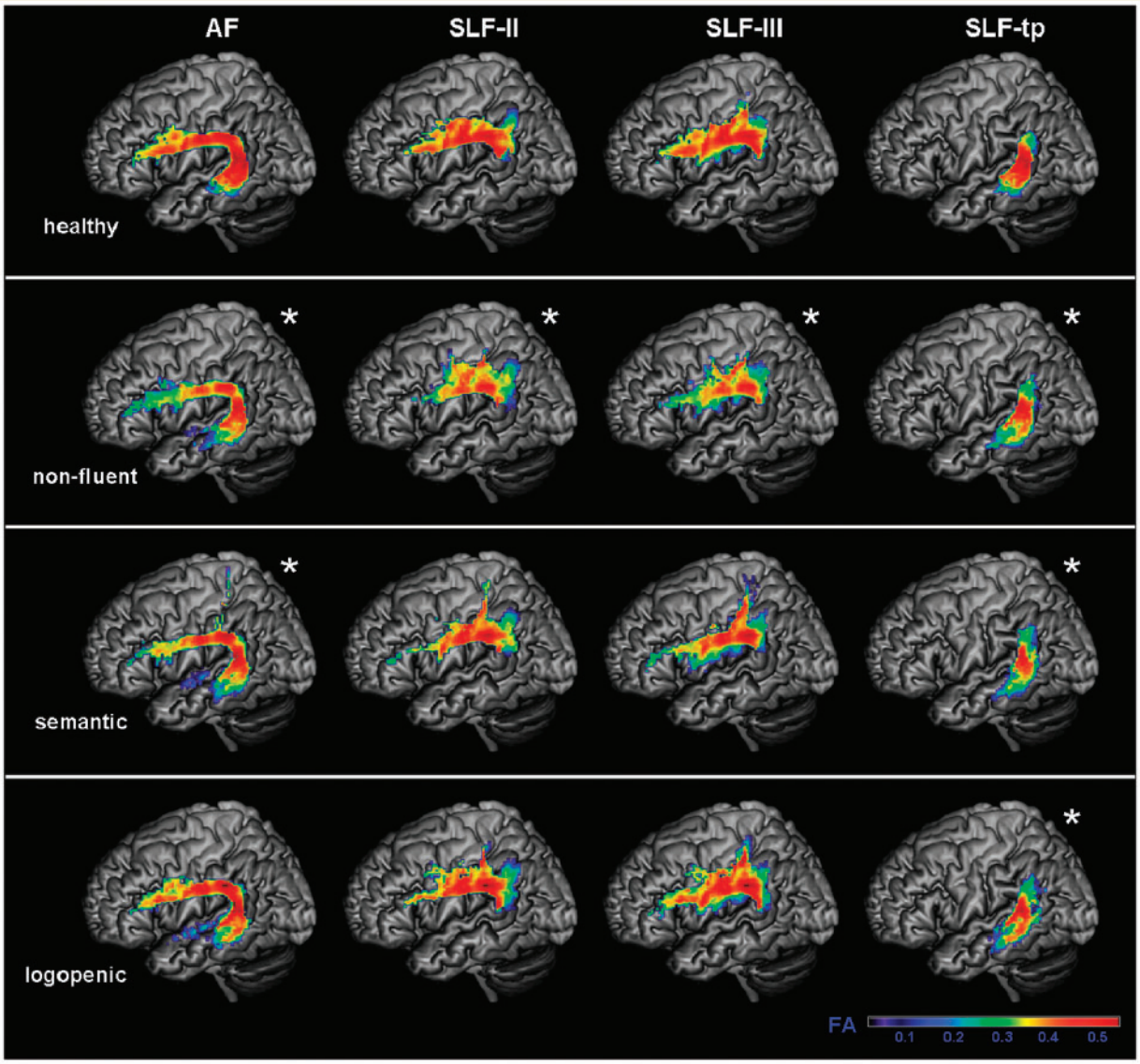

Figure 7 Fractional anisotropy values of each group in the probability maps for subcomponents of the left superior longitudinal fasciculus (SLF). Arcuate fasciculus (AF), frontoangular SLF (SLF-II), frontosupramarginal SLF (SLF-III) and temporoparietal SLF (SLF-tp) probability maps were overlaid on a standard MNI brain. Only voxels that are in common in at least 20% of the subjects in each group were included in the probability maps. Asterisk denotes significantly different relative to normal controls at $P < 0.05$. The chromatic scale represents average fractional anisotropy values, ranging from lower (violet–blue) to higher values (yellow–red).

When compared with non-fluent patients, semantic variant patients showed significantly lower fractional anisotropy values in left anterior inferior longitudinal fasciculus and bilateral uncinate fasciculus (Fig. 5). Mean diffusivity values were greater in semantic variant in bilateral anterior inferior longitudinal fasciculus, in left middle inferior longitudinal fasciculus and in bilateral uncinate fasciculus (Fig. 6). $\lambda//$ and $\lambda\perp$ values showed similar differences to mean diffusivity with the only exception of $\lambda//$ being increased in the left uncinate fasciculus.

In summary, this group showed damage in all DTI metrics bilaterally in the ventral tracts that connect the temporal lobe to the occipital lobe and to the orbitofrontal cortex, and in the left side, in tracts that connect the temporal lobe to the parietal and the frontal lobe. The dorsal frontoparietal tracts that do not involve the temporal lobes were spared bilaterally. The ventral pathways that involve the temporal lobes were damaged to a significantly greater extent in semantic variant compared with both the other primary progressive aphasia variants.

Logopenic variant

There was no difference in fractional anisotropy between logopenic patients and controls when entire tracts were considered (Fig. 5). However, when the different SLF components were analysed separately, the left temporoparietal portion showed significantly lower fractional anisotropy (Fig. 7). Mean diffusivity values

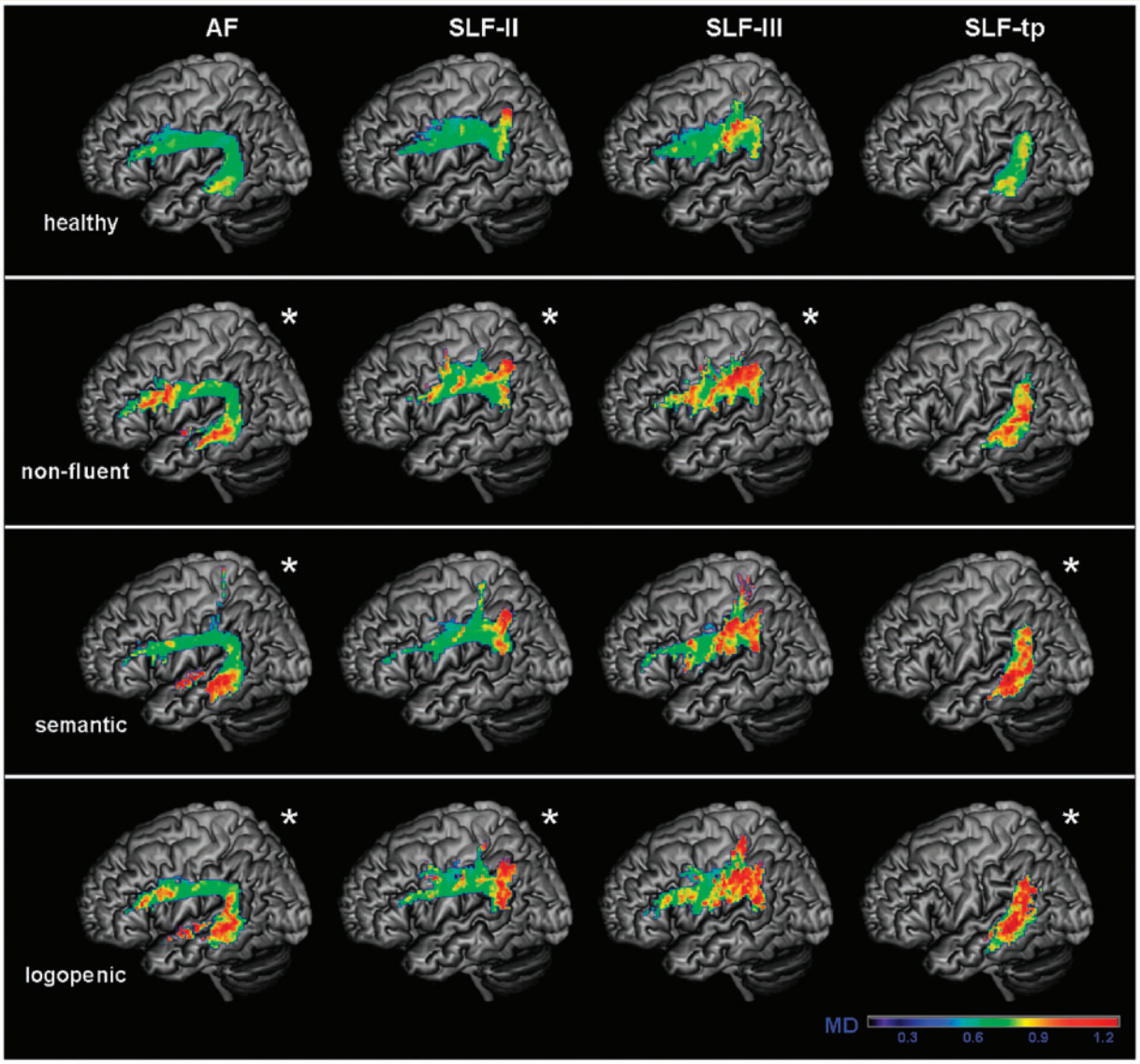

Figure 8 Mean diffusivity values of each group in the probability maps for subcomponents of the left superior longitudinal fasciculus (SLF). Arcuate fasciculus (AF), frontoangular SLF (SLF-II), frontosupramarginal SLF (SLF-III) and temporoparietal SLF (SLF-tp) probability maps were overlaid on a standard MNI brain. Only voxels that are in common in at least 20% of the subjects in each group were included in the probability maps. Asterisk denotes significantly different relative to normal controls at $P < 0.05$. The chromatic scale represents average mean diffusivity values, ranging from lower (violet–blue) to higher values (yellow–red). Mean diffusivity is measured in $mm^2/s \times 10^{-3}$.

were significantly higher in the entire left SLF of the patients with the logopenic variant, and also in their arcuate fasciculus, left SLF-II, and bilateral SLF-tp components (Figs 6 and 8). The logopenics' $\lambda//$ values showed a similar pattern to the mean diffusivity and were significantly higher in all the above-mentioned tracts and also in the left anterior inferior longitudinal fasciculus. The $\lambda\perp$ values were higher in the left arcuate fasciculus, left SLF-II and left SLF-tp.

When compared with logopenic patients, non-fluent patients showed lower fractional anisotropy in the entire left SLF and in the left SLF-III (Fig. 7). Diffusivity values did not differ. When compared with the logopenic group, the semantic patients showed lower fractional anisotropy in anterior inferior longitudinal fasciculus bilaterally and in uncinate fasciculus bilaterally (Fig. 5). Mean diffusivity was higher in the semantic variant patients in left anterior inferior longitudinal fasciculus, in the left middle inferior longitudinal fasciculus and in the uncinate fasciculus bilaterally (Fig. 6). $\lambda//$ values were increased in semantic variant in left anterior inferior longitudinal fasciculus and left uncinate fasciculus, while $\lambda\perp$ values were increased in semantic variant in anterior inferior longitudinal fasciculus bilaterally, in left middle inferior longitudinal fasciculus and in uncinate fasciculus bilaterally.

In summary, logopenic patients showed fractional anisotropy and diffusivity changes limited to the left temporoparietal

Table 1 Demographic and clinical data from healthy controls and patients with non-fluent, semantic and logopenic variants at the time of the MRI scan

	Healthy controls	Non-fluent variant	Semantic variant	Logopenic variant	Model
Age	65.3 (3.56)	66.6 (5.24)	62.5 (7.61)	61.6 (6.69)	NS
Gender (male/female)	8/13	3/6	3/6	5/4	NS
Education	17.3 (2.31)	15.1 (2.85)	15.7 (1.41)	15.7 (3.32)	NS
Handedness (left/right)	2/19	0/9	1/8	1/8	NS
Disease duration		4.1 (1.36)	5.8 (3.51)	4.1 (2.11)	NS
MMSE (30)	29.5 (0.68)	25.4 (4.44)*	19.1 (7.44)***	24.0 (6.06)**	***
CDR (boxes)		2.5 (2.33)	5.5 (3.21)	2.5 (2.00)	*

Values shown are mean (SD). Asterisks denote significantly impaired (or different) relative to healthy controls at $*P < 0.05$; $**P < 0.01$; $***P < 0.001$.
NS = not significant; CDR = Clinical Dementia Rating; MMSE = Mini-Mental State Examination.

Table 2 General cognitive functions on healthy controls (when available) and primary progressive aphasia subtypes

	Healthy controls	Non-fluent variant	Semantic variant	Logopenic variant	Model
Visuospatial function					
Modified Rey–Osterrieth copy (17)	15.1 (1.1)	14.8 (1.9)	15.6 (0.9)	15.0 (1.1)	NS
Visual memory					
Modified Rey–Osterrieth delay (17)	11.0 (2.6)	9.6 (3.2)	7.6 (5.9)	7.4 (2.7)	*
Rey recognition	1.0 (0.0)	0.6 (0.5)	0.8 (0.4)	0.7 (0.5)	*
Verbal memory					
CVLT-MS (30 s)		5.5 (2.7)	0.9 (1.4)[a,c]	4.7 (3.1)	**
CVLT-MS (10 min)		4.5 (2.7)	0.3 (0.5)[a,c]	4.3 (2.9)	**
CVLT-MS (recognition)		7.9 (1.4)	6.4 (1.7)	8.1 (1.1)	*
Executive function					
Digit span backwards	6.0 (1.3)	3.1 (1.4)***[,b]	5.0 (1.3)	3.2 (1.0)***[b]	***
Trails corrected lines per minute	37.2 (11.9)	28.1 (21.3)	22.9 (9.7)	15.2 (12.9)**	**
Calculation (5)	4.9 (0.3)	4.1 (1.4)	4.5 (0.5)	3.3 (0.9)***[b]	***

Values shown are mean (SD). Asterisks denote significantly impaired (or different) relative to healthy controls at $*P < 0.05$; $**P < 0.01$; $***P < 0.001$. Superscript letters denote significantly impaired (or different, in the case of demographic data) relative to the [a]non-fluent, [b]semantic and [c]logopenic variants at $P < 0.05$. Univariate ANOVAs were used to compare the different groups when not else specified.
CVLT-MS = California Verbal Learning Test-Mental Status; NS = not significant.

Table 3 Language functions on healthy controls (when available) and primary progressive aphasia subtypes

	Healthy controls	Non-fluent variant	Semantic variant	Logopenic variant	Model
Language production					
Boston naming test (15)	14.6 (0.7)	10.8 (4.5)*	1.7 (0.9)***[a,c]	10.0 (4.8)**	***
Phonemic fluency	18.1 (4.2)	5.8 (3.6)***	3.0 (2.6)***[c]	9.0 (5.9)***	***
Semantic fluency (animals)	23.19 (5.2)	9.0 (6.1)***	3.8 (3.0)***	9.1 (4.3)***	***
Speech fluency (WAB, 10)		5.0 (2.6)[a,b]	7.5 (1.2)	8.2 (1.7)	**
Repetition (WAB, 100)		80.0 (9.5)	76.4 (14.0)	72.2 (16.1)	NS
Motor speech					
Apraxia of speech rating (MSE, 7)		3.1 (2.0)b,c	0.0 (0.0)	0.0 (0.0)	***
Dysarthria rating (MSE, 7)		2.4 (3.2)b	0.0 (0.0)	0.0 (0.0)	*
Single-word comprehension and semantic function					
PPVT (16)	15.8 (0.4)	14.0 (2.1)	4.1 (2.8)***[a,c]	13.4 (2.4)*	***
Word recognition (WAB, 60)		59.1 (1.7)	47.7 (7.8)[a,c]	58.2 (3.5)	***
PPTP (52)		48.8 (2.4)	38.9 (8.5)[a,c]	50.0 (1.8)	***
Sentence comprehension					
CYCLE Raw		41.8 (8.6)	44.4 (9.7)	46.2 (5.8)	NS
CYCLE Per cent		75.8 (15.8)	80.6 (17.8)	83.8 (10.6)	NS

Values shown are mean (SD). Asterisks denote significantly impaired (or different) relative to healthy controls at $*P < 0.05$; $**P < 0.01$; $***P < 0.001$. Superscript letters denote significantly impaired (or different, in the case of demographic data) relative to the [a]non-fluent, [b]semantic and [c]logopenic variants at $P < 0.05$. Univariate ANOVAs were used to compare the different groups when not else specified.
CYCLE = Curtiss-Yamada Comprehensive Language Examination; MSE = Motor Speech Evaluation (Wertz *et al.*, 1984); PPTP = Pyramids and Palm trees pictures; PPVT = Peabody Picture Vocabulary Test; WAB = Western Aphasia Battery; NS = not significant.

Table 4 Group differences of regional fractional anisotropy in the tracts of interest

Tracts	Fractional anisotropy, mean (SD)				Model
	Healthy controls	Non-fluent variant	Semantic variant	Logopenic variant	
Left SLF	0.42 (0.02)	0.35 (0.03)***,c	0.39 (0.03)	0.4 (0.03)	***
Right SLF	0.40 (0.03)	0.37 (0.03)	0.39 (0.02)	0.39 (0.03)	NS
Left arcuate fasciculus	0.42 (0.03)	0.35 (0.03)***	0.37 (0.03)*	0.39 (0.03)	***
Right arcuate fasciculus	0.4 (0.02)	0.38 (0.04)	0.39 (0.03)	0.39 (0.02)	NS
Left SLF-II	0.41 (0.02)	0.36 (0.03)*	0.39 (0.04)	0.39 (0.02)	*
Right SLF-II	0.41 (0.02)	0.38 (0.04)	0.40 (0.03)	0.40 (0.02)	NS
Left SLF-III	0.38 (0.02)	0.34 (0.03)**,c	0.36 (0.03)	0.38 (0.02)	**
Right SLF-III	0.40 (0.03)	0.36 (0.04)	0.39 (0.03)	0.39 (0.02)	NS
Left SLF temporoparietal	0.36 (0.03)	0.29 (0.05)**	0.29 (0.05)**	0.31 (0.04)*	***
Right SLF temporoparietal	0.35 (0.03)	0.33 (0.02)	0.35 (0.04)	0.34 (0.04)	NS
Left inferior longitudinal fasciculus	0.36 (0.03)	0.35 (0.03)	0.31 (0.06)	0.35 (0.05)	NS
Right inferior longitudinal fasciculus	0.34 (0.03)	0.33 (0.04)	0.32 (0.03)	0.35 (0.04)	NS
Left anterior inferior longitudinal fasciculus	0.27 (0.03)	0.25 (0.03)	0.19 (0.04)***a,c	0.25 (0.03)	***
Right anterior inferior longitudinal fasciculus	0.28 (0.02)	0.26 (0.02)	0.23 (0.02)**,c	0.27 (0.02)	**
Left medial inferior longitudinal fasciculus	0.34 (0.03)	0.31 (0.03)	0.29 (0.04)*	0.34 (0.04)	*
Right med inferior longitudinal fasciculus	0.32 (0.03)	0.30 (0.03)	0.31 (0.03)	0.32 (0.03)	NS
Left post inferior longitudinal fasciculus	0.43 (0.04)	0.42 (0.03)	0.42 (0.04)	0.44 (0.03)	NS
Right post inferior longitudinal fasciculus	0.43 (0.04)	0.40 (0.05)	0.42 (0.04)	0.43 (0.03)	NS
Left uncinate fasciculus	0.31 (0.02)	0.29 (0.03)	0.22 (0.04)***a,c	0.30 (0.02)	***
Right uncinate fasciculus	0.33 (0.02)	0.31 (0.02)	0.27 (0.02)***a,c	0.32 (0.02)	***

Asterisks denote significantly impaired (or different) relative to healthy controls at $*P < 0.05$; $**P < 0.01$; $***P < 0.001$. Superscript letters denote significantly different relative to the [a]non-fluent, [b]semantic and [c]logopenic variants at $P < 0.05$.
NS = not significant.

Table 5 Group differences of regional mean diffusivity in the tracts of interest

Tracts	Mean diffusivity, mean (SD)				Model
	Healthy controls	Non-fluent variant	Semantic variant	Logopenic variant	
Left SLF	0.61 (0.03)	0.69 (0.06)**	0.65 (0.05)	0.67 (0.06)*	**
Right SLF	0.62 (0.04)	0.68 (0.05)	0.63 (0.04)	0.64 (0.03)	NS
Left arcuate fasciculus	0.61 (0.03)	0.70 (0.05)**	0.70 (0.07)**	0.68 (0.06)**	***
Right arcuate fasciculus	0.62 (0.03)	0.66 (0.06)	0.63 (0.03)	0.64 (0.04)	NS
Left SLF-II	0.61 (0.04)	0.68 (0.05)*	0.65 (0.05)	0.67 (0.05)*	**
Right SLF-II	0.61 (0.03)	0.66 (0.06)	0.62 (0.03)	0.63 (0.04)	*
Left SLF-III	0.64 (0.03)	0.70 (0.05)*	0.68 (0.04)	0.68 (0.04)	*
Right SLF-III	0.62 (0.03)	0.68 (0.05)	0.64 (0.04)	0.65 (0.02)	*
Left SLF temporoparietal	0.65 (0.03)	0.73 (0.08)	0.78 (0.10)***	0.74 (0.09)**	***
Right SLF temporoparietal	0.66 (0.03)	0.70 (0.05)	0.67 (0.05)	0.71 (0.07)*	*
Left inferior longitudinal fasciculus	0.65 (0.02)	0.69 (0.04)	0.82 (0.09)***a,c	0.71 (0.10)	***
Right inferior longitudinal fasciculus	0.65 (0.02)	0.67 (0.06)	0.71 (0.07)*	0.67 (0.04)	*
Left anterior inferior longitudinal fasciculus	0.68 (0.04)	0.73 (0.07)	0.97 (0.13)***a,c	0.76 (0.13)	***
Right anterior inferior longitudinal fasciculus	0.66 (0.04)	0.69 (0.06)	0.79 (0.11)**,a	0.69 (0.06)	**
Left medial inferior longitudinal fasciculus	0.61 (0.03)	0. 66 (0.04)	0.77 (0.09)***,a,c	0.67 (0.09)	***
Right medial inferior longitudinal fasciculus	0.63 (0.03)	0.66 (0.07)	0.68 (0.08)	0.64 (0.06)	NS
Left posterior inferior longitudinal fasciculus	0.67 (0.04)	0.68 (0.03)	0.72 (0.06)	0.69 (0.04)	NS
Right posterior inferior longitudinal fasciculus	0.65 (0.05)	0.66 (0.04)	0.67 (0.04)	0.67 (0.05)	NS
Left uncinate fasciculus	0.72 (0.03)	0.76 (0.05)	1.02 (0.19)***,a,c	0.77 (0.07)	***
Right uncinate fasciculus	0.70 (0.03)	0.73 (0.05)	0.81 (0.09)***a,c	0.72 (0.05)	***

Asterisks denote significantly impaired (or different) relative to healthy controls at $*P < 0.05$; $**P < 0.01$; $***P < 0.001$. Superscript letters denote significantly different relative to the [a]non-fluent, [b]semantic and [c]logopenic variants at $P < 0.05$. Mean diffusivity values are measured in $mm^2/s \times 10^{-3}$.
NS = not significant.

Table 6 Group differences of regional axial diffusivity λ// in the tracts of interest

Tracts	λ//, mean (SD)				Model
	Healthy controls	Non-fluent variant	Semantic variant	Logopenic variant	
Left SLF	0.89 (0.03)	0.95 (0.06)	0.92 (0.05)	0.95 (0.05)*	*
Right SLF	0.89 (0.03)	0.94 (0.05)	0.90 (0.04)	0.91 (0.03)	NS
Left arcuate fasciculus	0.89 (0.02)	0.95 (0.05)	0.96 (0.07)*	0.95 (0.06)*	**
Right arcuate fasciculus	0.89 (0.04)	0.94 (0.05)	0.90 (0.03)	0.91 (0.05)	NS
Left SLF-II	0.88 (0.04)	0.93 (0.05)	0.91 (0.05)	0.94 (0.05)**	**
Right SLF-II	0.87 (0.03)	0.93 (0.05)	0.89 (0.04)	0.90 (0.03)	*
Left SLF-III	0.89 (0.03)	0.94 (0.05)	0.93 (0.04)	0.94 (0.04)*	*
Right SLF-III	0.89 (0.03)	0.93 (0.05)	0.90 (0.04)	0.92 (0.02)	NS
Left SLF temporoparietal	0.90 (0.03)	0.94 (0.08)	1.00 (0.10)**	0.97 (0.08)*	**
Right SLF temporoparietal	0.90 (0.04)	0.95 (0.06)	0.92 (0.05)	0.96 (0.06)*	*
Left inferior longitudinal fasciculus	0.90 (0.04)	0.95 (0.04)	1.1 (0.07)***,a,c	0.98 (0.09)*	***
Right inferior longitudinal fasciculus	0.88 (0.04)	0.90 (0.05)	0.95 (0.08)*	0.91 (0.05)	*
Left anterior inferior longitudinal fasciculus	0.86 (0.05)	0.92 (0.07)	1.13 (0.12)***,a,c	0.95 (0.14)	***
Right anterior inferior longitudinal fasciculus	0.85 (0.04)	0.87 (0.06)	0.97 (0.12)**,a	0.88 (0.06)	**
Left medial inferior longitudinal fasciculus	0.83 (0.04)	0.87 (0.05)	0.99 (0.09)***,a	0.91 (0.10)*	***
Right medial inferior longitudinal fasciculus	0.83 (0.04)	0.85 (0.08)	0.89 (0.08)	0.84 (0.06)	NS
Left posterior inferior longitudinal fasciculus	1.00 (0.06)	1.01 (0.04)	1.08 (0.07)	1.04 (0.07)	*
Right posterior inferior longitudinal fasciculus	0.97 (0.07)	0.96 (0.04)	0.99 (0.08)	1.00 (0.05)	NS
Left uncinate fasciculus	0.96 (0.03)	0.99 (0.05)	1.24 (0.17)***,a,c	1.01 (0.07)	***
Right uncinate fasciculus	0.95 (0.03)	0.98 (0.06)	1.03 (0.08)**	0.96 (0.05)	**

Asterisks denote significantly impaired (or different) relative to healthy controls at $*P < 0.05$; $**P < 0.01$; $***P < 0.001$. Superscript letters denote significantly different relative to the [a]non-fluent, [b]semantic and [c]logopenic variants at $P < 0.05$. Values are measured in $mm^2/s \times 10^{-3}$.
NS = not significant.

Table 7 Group differences of regional radial diffusivity (λ⊥) in the tracts of interest

Tracts	Radial diffusivity (λ⊥), mean (SD)				Model
	Healthy controls	Non-fluent variant	Semantic variant	Logopenic variant	
Left SLF	0.47 (0.04)	0.57 (0.06)**	0.51 (0.05)	0.53 (0.06)	**
Right SLF	0.49 (0.04)	0.55 (0.05)	0.5 (0.04)	0.5 (0.04)	NS
Left arcuate fasciculus	0.47 (0,03)	0.57 (0.05)***	0.57 (0.08)**	0,54 (0.06)*	***
Right arcuate fasciculus	0.49 (0.02)	0.52 (0.06)	0.50 (0.04)	0.50 (0.04)	NS
Left SLF-II	0.48 (0.04)	055 (0.05)*	0.52 (0.06)	0.53 (0.05)*	**
Right SLF-II	0.47 (0.03)	0.53 (0.06)	0.49 (0.04)	0.50 (0.04)	NS
Left SLF-III	0.51 (0.04)	0.58 (0.05)*	0.56 (0.05)	0.54 (0.04)	**
Right SLF-III	0.49 (0.04)	0.55 (0.06)	0.50 (0.04)	0.52 (0.03)	*
Left SLF temporoparietal	0.52 (0.04)	0.62 (0.09)*	0.67 (0.11)***	0.63 (0.09)**	***
Right SLF temporoparietal	0.54 (0.04)	0.58 (0.05)	0.55 (0.05)	0.59 (0.08)	*
Left inferior longitudinal fasciculus	0.52 (0.03)	0.56 (0.04)	0.70 (0.10)***,a,c	0.58 (0.10)	***
Right inferior longitudinal fasciculus	0.53 (0.03)	0.55 (0.06)	0.59 (0.07)*	0.54 (0.05)	NS
Left anterior inferior longitudinal fasciculus	0.58 (0.04)	0.63 (0.07)	0.88 (0.13)***,a,c	0.67 (0.13)	***
Right anterior inferior longitudinal fasciculus	0.57 (0.03)	0.60 (0.06)	0.71 (0.12)**,a,c	0.59 (0.06)	**
Left medial inferior longitudinal fasciculus	0.50 (0.03)	0.55 (0.04)	0.66 (0.09)***,a,c	0.55 (0.09)	***
Right medial inferior longitudinal fasciculus	0.53 (0.03)	0.56 (0.07)	0.57 (0.08)	0.53 (0.06)	NS
Left posterior inferior longitudinal fasciculus	0.50 (0.04)	0.52 (0.03)	0.54 (0.07)	0.51 (0.03)	NS
Right posterior inferior longitudinal fasciculus	0.49 (0.05)	0.51 (0.05)	0.50 (0.04)	0.50 (0.06)	NS
Left uncinate fasciculus	0.60 (0.03)	0.64 (0.05)	0.92 (0.20)***,a,c	0.64 (0.07)	***
Right uncinate fasciculus	0.57 (0.03)	0.61 (0.05)	0.70 (0.07)***,a,c	0.60 (0.05)	***

Asterisks denote significantly impaired (or different) relative to healthy controls at $*P < 0.05$; $**P < 0.01$; $***P < 0.001$. Superscript letters denote significantly different relative to the [a]non-fluent, [b]semantic and [c]logopenic variants at $P < 0.05$. λ⊥ values are measured in $mm^2/s \times 10^{-3}$.
NS = not significant.

pathway. They also showed diffusivity only changes in other pathways of the dorsal network. No tract was more damaged in the logopenic variant than in the other variants.

Discussion

This study investigated white matter damage in the main language tracts and in their subcomponents in the three major variants of primary progressive aphasia using DTI tractography. Results showed that primary progressive aphasia variants are associated with significant white matter changes in specific networks that are fundamental to language processing. Furthermore, each variant showed a distinct pattern of alteration in the different DTI metrics considered.

Many previous studies that used DTI in neurodegenerative diseases have mainly considered fractional anisotropy values in voxels or tracts of interest (Chua *et al*., 2008; Matsuo *et al*., 2008; Damoiseaux *et al*., 2009; Mielke *et al*., 2009; Smith *et al*., 2010). In this study, we considered different tracts and their anatomical subcomponents, and also quantified other important DTI metrics such as axial, radial and mean diffusivity. Classically, decreases in fractional anisotropy have been used as a marker of myelin injury with axonal loss. This would result in sphere-like diffusion tensor, instead of the usual ellipsoid, because of increased radial diffusivity and a much smaller or no change in axial diffusivity. However, other situations, such as fibre reorganization, could occur in neurodegenerative disease resulting in a decrease in fractional anisotropy, but via a different mechanism, such as a reduction in axial diffusivity with an increase of radial diffusivity (Beaulieu, 2002; Song *et al*., 2002). Furthermore, other conditions such as glial alterations, increased membrane permeability and diffusivity, destruction of intracellular structures, alterations in the cytoskeleton and axonal transport, could influence different DTI metrics in ways that are not well understood (Beaulieu, 2002; Song *et al*., 2002). The presence of these pathological changes makes the understanding of the DTI alterations in neurodegenerative conditions complicated, but could explain, for instance, why fractional anisotropy changes are not always found (Agosta *et al*., 2009; Acosta-Cabronero *et al*., 2010). In this context, we discuss our findings of differential changes of the various DTI metrics in the specific language-related tracts in the primary progressive aphasia variants. We argue that our findings of differential anatomical and microstructural involvement warrant further investigation as possible markers of disease.

The non-fluent patients showed changes in DTI metrics in all the SLF components (Figs 5–8). Damage in this fundamental dorsal temporoparietal–frontal language tract and network was quite severe and might be partially responsible for some of the language features typical of this variant, such as motor speech difficulties and agrammatism. In comparison, the ventral tracts were relatively spared. The sparing of the inferior longitudinal fasciculus is consistent with these patients' good performance in single-word comprehension and semantic tasks. Interestingly, the uncinate was also spared in this variant, reflecting sparing of the anterior temporal to orbitofrontal network, which is possibly involved in behavioural and social functioning (Bramham *et al*., 2009) and in name retrieval (Papagno *et al*., 2011). A study by Rosen *et al*. (2006) showed that non-fluent patients had less behavioural symptoms than did those with the semantic variant.

When considering DTI metrics in the non-fluent variant, fractional anisotropy reduction and mean diffusivity increase were observed in all the tracts that showed significantly abnormal DTI results (SLF and its subcomponents, Figs 5–8). Axial diffusivity was never significantly different from controls, while radial diffusivity changes were present in all tracts that showed fractional anisotropy and mean diffusivity abnormalities. This pattern of DTI changes is suggestive of more severe myelin injury or a change in structures that create barriers for water diffusion along the direction perpendicular to the main axis of the axons. Only one previous study looked at DTI changes in the non-fluent variant (Whitwell *et al*., 2010). Using a region of interest-based approach, this study located abnormalities in the SLF, although tractography was not performed. No subcomponents of the different tracts were considered and relative changes in DTI metrics were not identified.

In summary, our DTI data showed that the non-fluent variant primary progressive aphasia is associated with severe white matter changes in the dorsal language network and this may be contributing to the phenotype. Clinicopathological correlation studies have shown that the non-fluent variant is most often, although not exclusively, associated with a tauopathy and in a minority of cases with TDP-43 type 3 Sampathu (Mackenzie type 1) (Josephs *et al*., 2006; Snowden *et al*., 2007; Yokota *et al*., 2009; Grossman, 2010). Progressive supranuclear palsy and corticobasal degeneration, classic tauopathies, both exhibit extensive glial pathology in white matter (Dickson *et al*., 2002; Zhukareva *et al*., 2006). Significant white matter pathology has also been reported in Pick's disease and in some areas was more extensive than in the adjacent grey matter (Zhukareva *et al*., 2002). Our findings of specific white matter changes in the non-fluent variant might thus be a marker of these pathological changes. Future pathological studies are needed to investigate this hypothesis.

Semantic variant patients showed severe involvement of the uncinate fasciculus bilaterally and of the inferior longitudinal fasciculus, especially the anterior portion bilaterally and the middle section in the left hemisphere (Figs 5 and 6). The components of the SLF that connect the temporal lobe to the dorsal language network (left arcuate fasciculus and temporoparietal component) were also involved, while the parietofrontal SLF components were relatively spared (Figs 7 and 8). A dysfunction of the ventral language system, with relative sparing of the dorsal network, accounts for the typical combination of impaired semantics and spared phonology, grammar and fluency language domains in semantic variant, as previously hypothesized (Agosta *et al*., 2009). The changes in the uncinate fasciculus might instead be related to the behavioural changes that often accompany language symptoms in semantic variant but the role of this tract is still debated (Papagno *et al*., 2011).

In the semantic variant, the tracts involved showed changes in all DTI metrics, including axial diffusivity, although radial diffusivity had the largest alteration, explaining the decrease of fractional anisotropy and the increase of mean diffusivity. Interestingly, as reported by Agosta and colleagues (2009) in a previous study of a

different group of semantic variant patients, fractional anisotropy did not change in the inferior longitudinal fasciculus when the tract was considered in its entirety, although mean diffusivity changes were evident (Figs 5 and 6). In our study, partitioning the inferior longitudinal fasciculus into anterior, middle and posterior portions revealed significant fractional anisotropy differences in the more anterior portions. Therefore, the less apparent change in fractional anisotropy with clear change in mean diffusivity in the entire inferior longitudinal fasciculus could be explained by the fact that pathology is most severe in the anterior temporal lobe and also by the particular pattern of DTI metrics changes, characterized by both axial and radial diffusivity increases.

In the semantic variant, the temporal lobe is so damaged that all tracts that connect to it are altered, including the left arcuate, consistent with previous studies (Kertesz *et al*., 2005; Seeley *et al*., 2005; Borroni *et al*., 2007; Snowden *et al*., 2007; Grossman *et al*., 2008; Agosta *et al*., 2009; Brambati *et al*., 2009; Whitwell *et al*., 2010). DTI changes decreased in severity while moving posteriorly along the inferior longitudinal fasciculus, with the left middle portion showing significant fractional anisotropy and mean diffusivity differences and the most posterior portion showing only a trend for axial diffusivity increase. The anterior–posterior axis of decreased severity in white matter changes is consistent with previous grey matter longitudinal findings showing atrophy moving posteriorly and contralaterally as disease progresses (Brambati *et al*., 2009). The changes in all DTI metrics suggest that the white matter injury in semantic patients may be more severe than in non-fluent and logopenic patients, especially in the anterior temporal regions where ventral language and behavioural pathways relay in the temporal lobe. As in the case of the non-fluent variant, these changes are likely to be primary contributors to the disease process, together with grey matter changes.

Clinicopathological correlations have shown that the semantic variant clinical syndrome is reliably associated with frontotemporal lobar degeneration-TDP pathology (Kertesz *et al*., 2005; Snowden *et al*., 2007), almost invariably Sampathu frontotemporal lobar degeneration-TDP 1 (Mackenzie type 2) (Mackenzie *et al*., 2006; Sampathu *et al*., 2006). Frontal and temporal lobe white matter pathology has been seen in the three frontotemporal lobar degeneration-TDP subtypes (Neumann *et al*., 2007). TDP-43-positive glial inclusions were found in the frontal and temporal lobes and these inclusions were thought to occur in oligodendrocytes. In a small study, Tartaglia *et al*. (2010) investigated more extensively the distribution of the pathology in the three frontotemporal lobar degeneration-TDP subtypes and found that affected white matter regions showed reduced myelin staining, axonal loss, reactive gliosis, microglial activation and TDP-43 glial inclusions and threads. The degree of white matter pathology varied significantly among cases and across different anatomical regions. Frontotemporal lobar degeneration-TDP 3 (Mackenzie type 1) cases with clinical syndromes of behavioural frontotemporal dementia and non-fluent variant primary progressive aphasia showed the greatest white matter degeneration in the deep frontal lobe. In cases with frontotemporal lobar degeneration-TDP 1 (Mackenzie type 2), all having semantic variant primary progressive aphasia, the anterior temporal lobe white matter showed the most damage. Cases with frontotemporal lobar degeneration-TDP 2 (MacKenzie type 3) had the least white matter degeneration with frontal and anterior temporal regions equally affected. The degree of reduced myelin staining and axonal loss correlated strongly. Cases with frontotemporal lobar degeneration-TDP 3 (Mackenzie type 1) had the most white matter TDP-43 pathology; however, this did not correlate with degree of white matter degeneration. The extensive white matter pathology suggests that glial TDP-43 white matter pathology is a characteristic feature of frontotemporal lobar degeneration-TDP and that glial TDP-43 pathology also contributes to the neurodegenerative process and the cognitive and motor impairments seen in patients affected by frontotemporal lobar degeneration-TDP. Our results, together with previous evidence, suggest that DTI might become an *in vivo* marker of this process.

Logopenic patients showed the most consistent DTI changes in the left SLF temporoparietal component, but also abnormalities in the left arcuate fasciculus, in SLF-II and III and in the right temporoparietal SLF (Figs 7 and 8). These results are consistent with volumetric studies demonstrating grey matter atrophy and demonstrate how patients with the logopenic variant have involvement of tracts that connect regions important for sentence repetition and phonological short-term memory (Gorno-Tempini *et al*., 2008; Hu *et al*., 2010).

A close look at the pattern of change in the DTI metrics in logopenic patients revealed that the temporoparietal component of the left SLF was the most injured with all DTI metrics showing significant changes. The fractional anisotropy was significantly lower than in controls because of a larger increase of radial than axial diffusivity (Fig. 7). Mean diffusivity was altered in left frontoangular SLF (SLF-II) and arcuate fasciculus as well as the right temporoparietal SLF (Fig. 8). Radial diffusivity showed changes that paralleled the mean diffusivity increase in these tracts, while only axial diffusivity was altered in the left SLF-III and left middle inferior longitudinal fasciculus. One interpretation is that the only tract that showed changes on the shape of the diffusion ellipsoid (temporoparietal SLF), could be the most damaged, as demyelination and axonal loss could be at play. The rest of the dorsal language network showed only diffusivity increases but no change in fractional anisotropy, suggesting less severe damage without disruption of directionality.

Taken together, these results suggest that diffusivities, including axial and radial diffusivity as well as their average may be more sensitive than fractional anisotropy to the pathological changes occurring in logopenic variant. Interestingly, similar qualitative DTI results were demonstrated, even if in different tracts or regions, in patients with early Alzheimer's disease suggesting that absolute diffusivities were more sensitive than fractional anisotropy in defining the white matter damage in these patients (Acosta-Cabronero *et al*., 2010). Several studies have shown that the logopenic variant is most often associated with Alzheimer's disease pathology (Grossman *et al*., 2008; Josephs *et al*., 2008; Mesulam *et al*., 2008) and Pittsburgh compound B-positive PET scans (Rabinovici *et al*., 2008). It has also been suggested that the logopenic variant is a left-lateralized form of early-age-of-onset Alzheimer's disease thus explaining why these patients have DTI changes similar to those already described for

Alzheimer's disease but in a language-related location (Migliaccio *et al*., 2009). In support of this hypothesis, seven out of eight of the logopenic patients included in this study had a positive Pittsburgh compound B scan.

Pathologically, Alzheimer's disease is also associated with white matter damage but seemingly of a different nature than in frontotemporal lobar degeneration. Two types of white matter pathology have been observed in Alzheimer's disease, excluding the vascular changes related to infarcts and ischaemia: Wallerian degeneration and white matter disease (Englund, 1998). Wallerian degeneration, a secondary phenomenon, tends to be seen adjacent to the atrophied grey matter. The white matter was atrophied and the tissue rarefied and collapsed when the disease was advanced. The temporal lobes had the greatest amount of white matter changes but this was present in a milder form elsewhere. They noted a mild decrease of axons, myelin and oligodendrocytes with some astrocytosis and the pathology was symmetrical. The second type of white matter pathological change was white matter rarefaction related to an angiopathy in the deep hemispheric regions. It had a preferential location in the frontal lobes and did not follow the regional extension of the grey matter changes. They observed a decrease in myelin with a parallel decrease in axonal density. They saw a partial loss of oligodendrocytes and the vessels showed a hyalinized sclerosis. Some patients with Alzheimer's disease showed both types of white matter injury and others showed one or the other. Amyloid plaques have been described in the white matter, most adjacent to the grey matter but at a considerable distance (Braak *et al*., 1989). The different and maybe less primary damage of white matter pathology in Alzheimer's disease could contribute to the different patterns of DTI changes that we observed in our logopenic patients.

Our study therefore indicates that each primary progressive aphasia clinical phenotype shows different patterns of white matter damage with focal involvement of specific portions of the language pathways and that these changes can be assessed using DTI. Different patterns of changes in DTI metrics observed in the different groups likely reflected differences in the underlying biological and pathological process. The precise relationship between the different pathological substrates seen in primary progressive aphasia patients and the different DTI metrics is currently unknown. One could speculate that post-mortem radiological–pathological studies will reveal patterns associated with primary progressive aphasia that could be used for *in vivo* diagnosis of the specific molecular pathology. Hence, beyond subtype tracking, DTI could play a role as an *in vivo* biomarker of specific molecular pathologies. This would be particularly important when treatments directed at specific molecular pathologies become available.

There are limitations in this study mainly related to the use of a diffusion tensor-based technique. One issue relates to the undetermined influence that tissue pathology can have on the correct alignment of the major eigenvector with the axons of the underlying white matter (Wheeler-Kingshott and Cercignani, 2009). This concern is somewhat mitigated by the fact that imperfect alignment of eigenvectors should not influence fractional anisotropy and mean diffusivity. Another limitation is that the diffusion tensor model deals poorly with crossing fibres, which result in a more spherical shape of the diffusion tensor ellipsoid, even in the absence of white matter damage. This limitation could be an issue and could make tractography less accurate, for instance, when we separate the SLF into the different components, resulting in a partial overlap between the components. The last issue is that our results lack post-mortem pathological–radiological correlations that would be required to definitively relate biological substrates to the changes in the various DTI metrics.

In conclusion, this is the first study to compare the three main variants of primary progressive aphasia using DTI tractography. The results demonstrate that distinct patterns of white matter alteration occur in the three primary progressive aphasia subtypes at both anatomical and micro-structural levels. How these changes are related to different pathological substrates has yet to be established.

Acknowledgements

We thank Elisabetta Pagani for helpful discussions; Robin Ketelle, Matthew Growdon, Jung Jang and Robert Nicholson for administrative support; and patients, caregivers and volunteers for their participation in our research.

Funding

National Institutes of Health (NINDS R01 NS050915, NIA P50 AG03006, NIA P01 AG019724); State of California (DHS 04-35516); Alzheimer's Disease Research Centre of California (03-75271 DHS/ADP/ARCC); Larry L. Hillblom Foundation; John Douglas French Alzheimer's Foundation; Koret Family Foundation; and McBean Family Foundation.

Supplementary material

Supplementary material is available at *Brain* online.

References

Acosta-Cabronero J, Williams GB, Pengas G, Nestor PJ. Absolute diffusivities define the landscape of white matter degeneration in Alzheimer's disease. Brain 2010; 133: 529–39.

Agosta F, Henry RG, Migliaccio R, Neuhaus J, Miller BL, Dronkers NF, et al. Language networks in semantic dementia. Brain 2009; 133: 286–99.

Ashburner J, Friston KJ. Unified segmentation. Neuroimage 2005; 26: 839–51.

Ashburner J. A fast diffeomorphic image registration algorithm. Neuroimage 2007; 38: 95–113.

Assaf Y, Pasternak O. Diffusion tensor imaging (DTI)-based white matter mapping in brain research: a review. J Mol Neurosci 2008; 34: 51–61.

Basser PJ, Mattiello J, LeBihan D. MR diffusion tensor spectroscopy and imaging. Biophys J 1994; 66: 259–67.

Beaulieu C. The basis of anisotropic water diffusion in the nervous system - a technical review. NMR Biomed 2002; 15: 435–55.

Behrens TE, Woolrich MW, Jenkinson M, Johansen-Berg H, Nunes RG, Clare S, et al. Characterization and propagation of uncertainty in diffusion-weighted MR imaging. Magn Reson Med 2003; 50: 1077–88.

Behrens TE, Berg HJ, Jbabdi S, Rushworth MF, Woolrich MW. Probabilistic diffusion tractography with multiple fibre orientations: what can we gain? Neuroimage 2007; 34: 144–55.

Borroni B, Brambati SM, Agosti C, Gipponi S, Bellelli G, Gasparotti R, et al. Evidence of white matter changes on diffusion tensor imaging in frontotemporal dementia. Arch Neurol 2007; 64: 246–51.

Braak H, Braak E, Kalus P. Alzheimer's disease: areal and laminar pathology in the occipital isocortex. Acta Neuropathol 1989; 77: 494–506.

Brambati SM, Rankin KP, Narvid J, Seeley WW, Dean D, Rosen HJ, et al. Atrophy progression in semantic dementia with asymmetric temporal involvement: a tensor-based morphometry study. Neurobiol Aging 2009; 30: 103–11.

Bramham J, Morris RG, Hornak J, Bullock P, Polkey C.E. Social and emotional functioning following bilateral and unilateral neurosurgical prefrontal cortex lesions. J Neuropsychol 2009; 3: 125–43.

Catani M, Howard RJ, Pajevic S, Jones DK. Virtual in vivo interactive dissection of white matter fasciculi in the human brain. Neuroimage 2002; 17: 77–94.

Catani M, Jones DK, ffytche DH. Perisylvian language networks of the human brain. Ann Neurol 2005; 57: 8–16.

Catani M, Thiebaut de Schotten M. A diffusion tensor imaging tractography atlas for virtual in vivo dissections. Cortex 2008; 44: 1105–32.

Chua TC, Wen W, Slavin MJ, Sachdev PS. Diffusion tensor imaging in mild cognitive impairment and Alzheimer's disease: a review. Curr Opin Neurol 2008; 21: 83–92.

Croxson PL, Johansen-Berg H, Behrens TE, Robson MD, Pinsk MA, Gross CG, et al. Quantitative investigation of connections of the prefrontal cortex in the human and macaque using probabilistic diffusion tractography. J Neurosci 2005; 25: 8854–66.

Damoiseaux JS, Smith SM, Witter MP, Sanz-Arigita EJ, Barkhof F, Scheltens P, et al. White matter tract integrity in aging and Alzheimer's disease. Hum Brain Mapp 2009; 30: 1051–9.

Davies RR, Hodges JR, Kril JJ, Patterson K, Halliday GM, Xuereb JH. The pathological basis of semantic dementia. Brain 2005; 128: 1984–95.

Dickson DW, Bergeron C, Chin SS, Duyckaerts C, Horoupian D, Ikeda K, et al. Office of Rare Diseases neuropathologic criteria for corticobasal degeneration. J Neuropathol Exp Neurol 2002; 61: 935–46.

Englund E. Neuropathology of white matter changes in Alzheimer's disease and vascular dementia. Dement Geriatr Cogn Disord 1998; 9 (Suppl 1): 6–12.

Frey S, Campbell JS, Pike GB, Petrides M. Dissociating the human language pathways with high angular resolution diffusion fiber tractography. J Neurosci 2008; 28: 11435–44.

Friederici AD, Bahlmann J, Heim S, Schubotz RI, Anwander A. The brain differentiates human and non-human grammars: functional localization and structural connectivity. Proc Natl Acad Sci USA 2006; 103: 2458–63.

Glasser MF, Rilling JK. DTI tractography of the human brain's language pathways. Cereb Cortex 2008; 18: 2471–82.

Gorno-Tempini ML, Dronkers NF, Rankin KP, Ogar JM, Phengrasamy L, Rosen HJ, et al. Cognition and anatomy in three variants of primary progressive aphasia. Ann Neurol 2004; 55: 335–46.

Gorno-Tempini ML, Brambati SM, Ginex V, Ogar J, Dronkers NF, Marcone A, et al. The logopenic/phonological variant of primary progressive aphasia. Neurology 2008; 71: 1227–34.

Gorno-Tempini ML, Hillis AE, Weintraub S, Kertesz A, Mendez MF, Cappa SF, et al. Classification of primary progressive aphasia and its variants. Neurology 2011; 76: 1006–14.

Grossman M, Xie SX, Libon DJ, Wang X, Massimo L, Moore P, et al. Longitudinal decline in autopsy-defined frontotemporal lobar degeneration. Neurology 2008; 70: 2036–45.

Grossman M. Primary progressive aphasia: clinicopathological correlations. Nat Rev Neurol 2010; 6: 88–97.

Hagmann P, Jonasson L, Maeder P, Thiran JP, Wedeen VJ, Meuli R. Understanding diffusion MR imaging techniques: from scalar diffusion-weighted imaging to diffusion tensor imaging and beyond. Radiographics 2006; 26 (Suppl 1): S205–23.

Henry ML, Gorno-Tempini ML. The logopenic variant of primary progressive aphasia. Curr Opin Neurol 2010; 23: 633–7.

Hodges JR, Patterson K. Nonfluent progressive aphasia and semantic dementia: a comparative neuropsychological study. J Int Neuropsychol Soc 1996; 2: 511–24.

Hu WT, McMillan C, Libon D, Leight S, Forman M, Lee VM, et al. Multimodal predictors for Alzheimer disease in nonfluent primary progressive aphasia. Neurology 2010; 75: 595–602.

Josephs KA, Duffy JR, Strand EA, Whitwell JL, Layton KF, Parisi JE, et al. Clinicopathological and imaging correlates of progressive aphasia and apraxia of speech. Brain 2006; 129: 1385–98.

Josephs KA, Whitwell JL, Duffy JR, Vanvoorst WA, Strand EA, Hu WT, et al. Progressive aphasia secondary to Alzheimer disease vs FTLD pathology. Neurology 2008; 70: 25–34.

Kertesz A, McMonagle P, Blair M, Davidson W, Munoz DG. The evolution and pathology of frontotemporal dementia. Brain 2005; 128: 1996–2005.

Knibb JA, Xuereb JH, Patterson K, Hodges JR. Clinical and pathological characterization of progressive aphasia. Ann Neurol 2006; 59: 156–65.

Mackenzie IR, Shi J, Shaw CL, Duplessis D, Neary D, Snowden JS, et al. Dementia lacking distinctive histology (DLDH) revisited. Acta Neuropathol 2006; 112: 551–9.

Makris N, Worth AJ, Sorensen AG, Papadimitriou GM, Wu O, Reese TG, et al. Morphometry of in vivo human white matter association pathways with diffusion-weighted magnetic resonance imaging. Ann Neurol 1997; 42: 951–62.

Makris N, Kennedy DN, McInerney S, Sorensen AG, Wang R, Caviness VS, et al. Segmentation of subcomponents within the superior longitudinal fascicle in humans: a quantitative, in vivo, DT-MRI study. Cereb Cortex 2005; 15: 854–69.

Makris N, Papadimitriou GM, Kaiser JR, Sorg S, Kennedy DN, Pandya DN. Delineation of the middle longitudinal fascicle in humans: a quantitative, in vivo, DT-MRI study. Cereb Cortex 2009; 19: 777–85.

Matsuo K, Mizuno T, Yamada K, Akazawa K, Kasai T, Kondo M, et al. Cerebral white matter damage in frontotemporal dementia assessed by diffusion tensor tractography. Neuroradiology 2008; 50: 605–11.

Mesulam M, Wicklund A, Johnson N, Rogalski E, Leger GC, Rademaker A, et al. Alzheimer and frontotemporal pathology in subsets of primary progressive aphasia. Ann Neurol 2008; 63: 709–19.

Mesulam M, Wieneke C, Rogalski E, Cobia D, Thompson C, Weintraub S. Quantitative template for subtyping primary progressive aphasia. Arch Neurol 2009; 66: 1545–51.

Mesulam MM. Slowly progressive aphasia without generalized dementia. Ann Neurol 1982; 11: 592–8.

Mesulam MM. Primary progressive aphasia. Ann Neurol 2001; 49: 425–32.

Mielke MM, Kozauer NA, Chan KC, George M, Toroney J, Zerrate M, et al. Regionally-specific diffusion tensor imaging in mild cognitive impairment and Alzheimer's disease. Neuroimage 2009; 46: 47–55.

Migliaccio R, Agosta F, Rascovsky K, Karydas A, Bonasera S, Rabinovici GD, et al. Clinical syndromes associated with posterior atrophy: early age at onset AD spectrum. Neurology 2009; 73: 1571–8.

Mummery CJ, Patterson K, Price CJ, Ashburner J, Frackowiak RS, Hodges JR. A voxel-based morphometry study of semantic dementia: relationship between temporal lobe atrophy and semantic memory. Ann Neurol 2000; 47: 36–45.

Neary D, Snowden JS, Gustafson L, Passant U, Stuss D, Black S, et al. Frontotemporal lobar degeneration: a consensus on clinical diagnostic criteria. Neurology 1998; 51: 1546–54.

Neumann M, Kwong LK, Truax AC, Vanmassenhove B, Kretzschmar HA, Van Deerlin VM, et al. TDP-43-positive white matter pathology in frontotemporal lobar degeneration with ubiquitin-positive inclusions. J Neuropathol Exp Neurol 2007; 66: 177–83.

Papagno C, Miracapillo C, Casarotti A, Romero Lauro LJ, Castellano A, Falini A, et al. What is the role of the uncinate fasciculus? Surgical removal and proper name retrieval. Brain 2011; 134: 405–14.

Rabinovici GD, Furst AJ, O'Neil JP, Racine CA, Mormino EC, Baker SL, et al. 11 C-PIB PET imaging in Alzheimer disease and frontotemporal lobar degeneration. Neurology 2007; 68: 1205–12.

Rabinovici GD, Jagust WJ, Furst AJ, Ogar JM, Racine CA, Mormino EC, et al. Abeta amyloid and glucose metabolism in three variants of primary progressive aphasia. Ann Neurol 2008; 64: 388–401.

Rabinovici GD, Miller BL. Frontotemporal lobar degeneration: epidemiology, pathophysiology, diagnosis and management. CNS Drugs 2010; 24: 375–98.

Rilling JK, Glasser MF, Preuss TM, Ma X, Zhao T, Hu X, et al. The evolution of the arcuate fasciculus revealed with comparative DTI. Nat Neurosci 2008; 11: 426–8.

Rosen HJ, Allison SC, Ogar JM, Amici S, Rose K, Dronkers N, et al. Behavioral features in semantic dementia vs other forms of progressive aphasias. Neurology 2006; 67: 1752–6.

Sampathu DM, Neumann M, Kwong LK, Chou TT, Micsenyi M, Truax A, et al. Pathological heterogeneity of frontotemporal lobar degeneration with ubiquitin-positive inclusions delineated by ubiquitin immunohistochemistry and novel monoclonal antibodies. Am J Pathol 2006; 169: 1343–52.

Seeley WW, Bauer AM, Miller BL, Gorno-Tempini ML, Kramer JH, Weiner M, et al. The natural history of temporal variant frontotemporal dementia. Neurology 2005; 64: 1384–90.

Smith CD, Chebrolu H, Andersen AH, Powell DA, Lovell MA, Xiong S, et al. White matter diffusion alterations in normal women at risk of Alzheimer's disease. Neurobiol Aging 2010; 31: 1122–31.

Snowden J, Neary D, Mann D. Frontotemporal lobar degeneration: clinical and pathological relationships. Acta Neuropathol 2007; 114: 31–8.

Song SK, Sun SW, Ramsbottom MJ, Chang C, Russell J, Cross AH. Dysmyelination revealed through MRI as increased radial (but unchanged axial) diffusion of water. Neuroimage 2002; 17: 1429–36.

Tartaglia M, Luk M, Miller B, Mackenzie IR. White Matter Pathology in FTLD-TDP. Dement Geriatr Cogn Disord 2010; 30: 85.

Wheeler-Kingshott CA, Cercignani M. About "axial" and "radial" diffusivities. Magn Reson Med 2009; 61: 1255–60.

Whitwell JL, Avula R, Senjem ML, Kantarci K, Weigand SD, Samikoglu A, et al. Gray and white matter water diffusion in the syndromic variants of frontotemporal dementia. Neurology 2010; 74: 1279–87.

Wilson SM, Ogar JM, Laluz V, Growdon M, Jang J, Glenn S, et al. Automated MRI-based classification of primary progressive aphasia variants. Neuroimage 2009; 47: 1558–67.

Yamada K, Sakai K, Akazawa K, Yuen S, Nishimura T. MR tractography: a review of its clinical applications. Magn Reson Med Sci 2009; 8: 165–74.

Yokota O, Tsuchiya K, Arai T, Yagishita S, Matsubara O, Mochizuki A, et al. Clinicopathological characterization of Pick's disease versus frontotemporal lobar degeneration with ubiquitin/TDP-43-positive inclusions. Acta Neuropathol 2009; 117: 429–44.

Zhang Y, Schuff N, Du AT, Rosen HJ, Kramer JH, Gorno-Tempini ML, et al. White matter damage in frontotemporal dementia and Alzheimer's disease measured by diffusion MRI. Brain 2009; 132: 2579–92.

Zhukareva V, Mann D, Pickering-Brown S, Uryu K, Shuck T, Shah K, et al. Sporadic Pick's disease: a tauopathy characterized by a spectrum of pathological tau isoforms in gray and white matter. Ann Neurol 2002; 51: 730–9.

Zhukareva V, Joyce S, Schuck T, Van Deerlin V, Hurtig H, Albin R, et al. Unexpected abundance of pathological tau in progressive supranuclear palsy white matter. Ann Neurol 2006; 60: 335–45.